JPL D-13315
Contract Data Requirements List (CDRL) #98

Earth Observing System

Multi-angle Imaging Spectro-Radiometer

In-Flight Radiometric Calibration and Characterization Plan

Carol Bruegge[1]
Robert Woodhouse[1]

[1]Jet Propulsion Laboratory, California Institute of Technology

Jet Propulsion Laboratory
California Institute of Technology

April 29, 1996

JPL D-13315

Multi-angle Imaging SpectroRadiometer (MISR)

In-Flight Radiometric Calibration and Characterization Plan

Approvals:

David J. Diner
MISR Principal Investigator

Terrence H. Reilly
MISR Project Manager

Graham W. Bothwell
MISR Science Data System Manager

James E. Conel
MISR Validation Scientist

Jet Propulsion Laboratory
California Institute of Technology

TABLE OF CONTENTS

ACRONYMS

A

ARP	Ancillary Radiometric Product
AVIRIS	Airborne Visible/ Infrared Imaging Spectrometer
AΩ	detector area times field-of-view product

B

BLS	baseline stabilization
BRF	bidirectional reflectance function

C

CAM	Calibration Attitude Maneuvers
CAT	Collimator Array Tool
CCD	Charge-Coupled Device
CTE	charge transfer efficiency

D

DAAC	Distributed Active Archive Center
DN	digital number

E

EOS	Earth Observing System

F

FFT	Fast Fourier Transform
FIFE	First ISLSCP Field Experiment

G

GSFC	Goddard Space Flight Center

H

HE	histogram equalization
HE	histogram equilization
HQE	High Quantum Efficiency

I

IFOV	instantaneous field-of-view
IFRCC	In-Flight Radiometric Calibration and Characterization
ISLSCP	International Satellite Land Surface Climatology Project

J

JPL	Jet Propulsion Laboratory

L

LM	Local Mode

M

MAST	MISR Aliveness and Stability Test

MISR	Multi-angle Imaging SpectroRadiometer
MODIS	Moderate Resolution Imaging Spectroradiometer
MSS	Multispectral Scanner System
MTF	modulation transfer function

N

NIST	National Institute of Standards and Technology
NRLM	National Research Laboratory of Metrology

O

OBC	On-Board Calibrator
OCC	Optical Characterization Chamber

P

PAR	photosynthetically active radiation
PIN	stacked p, intrinsic, and n doped layers
PGS	Product Generation System
PSF	point-spread-function
PTFE	polytetrafluoroethylene

Q

QA	quality assessment

R

RCC	Radiometric Characterization Chamber
RTC	radiative transfer code

S

SCF	Science Computing Facility
SNR	signal-to-noise ratio
SPOT	Système Probatoire d'Observation de la Terre

T

TDRSS	Tracking and Data Relay Satellite System
TM	Thematic Mapper
TOA	top-of-atmosphere

U

UV	ultraviolet

V

VC	vicarious calibration

1. INTRODUCTION

1.1 PURPOSE

This document defines the strategy for producing the in-flight radiometric calibration and characterization (IFRCC) of the Multi-angle Imaging SpectroRadiometer (MISR). The effort will be managed by the MISR Instrument Scientist and implemented by the IFRCC team, which resides at NASA/ Jet Propulsion Laboratory (JPL), and will draw upon other MISR resources as needed to accomplish its objectives. The activities can be divided into two major sub-tasks: 1) the development of algorithms and software for the analysis and archival of data in order to maintain the calibration and monitor performance metrics of the instrument, and 2) the development of algorithms needed for the production of the MISR Level 1B1 Radiometric Product.

1.2 SCOPE

This plan is divided into nine sections.

- Section 1 provides the purpose and scope of the document, and lists MISR Project documents relevant to this plan.

- Section 2 gives an overview of the MISR experiment, instrument, and data products.

- Section 3 is an overview of the in-flight radiometric calibration and characterization approach and objectives.

- Section 4 is a description of those preflight test activities that provide heritage to this in-flight program. Included is a summary of camera performance issues that have impacted the Level 1B1 processing approach and anticipated data anomaly conditions..

- Section 5 provides a detailed description of the in-flight radiometric calibration methodologies, including the derivation of coefficients and radiance uncertainties from On-Board Calibrator (OBC), vicarious calibration (VC), histogram equalization (HE), and trend data sets.

- Section 6 provides an overview of the processing algorithms and Ancillary Radiometric Product (ARP) input used to provide the MISR Level 1B1 Radiometric Product. These algorithms are used to retrieve incident radiances, given camera digital numbers (DN).

- Section 7 describes the plans to provide the instrument characterization. Here, instrument performance is studied under specific viewing conditions which may affect the data quality. Included in this task is the determination of radiometric uncertainties for specific scene types, and the noise assessment of the data.

- Section 8 describes the calibration integrity task. The primary objective of this task is the validation of the Level 1B1 Radiometric Product. Sensor cross-comparisons are made, and lunar observation data are tracked (if available) as part of the radiometric calibration verification program. Additionally, this section covers quality assessment and traceability of the radiance scale.

- Section 9 is the management description, including personnel and computing resources, and the top-level schedule.

- Section 10 provides open-literature references from peer-reviewed and conference publications.

The appendices provide:

- IFRCC nomenclature; and

- details of the on-orbit calibration mode sequences.

1.3 APPLICABLE DOCUMENTS

Throughout this document a notation of the form [shorthand] will be used to reference project documents. The actual references and associated [shorthand] definitions are listed in Sections 1.3.1 and 1.3.2. Open literature references are pointed to by means of superscript numbers in the text. These numbers refer to the publications listed in Chapter 10.

Other MISR calibration activities are described elsewhere. Specifically, the preflight calibration plan is described in [PreCal Plan]; and in-flight geometric calibration is described in [GeoCal Plan]. The latter activity is required for generation of the Level 1B2 Georectified Radiance Product. The provision of top-of-atmosphere vicarious radiances across the spectrum at MISR view angles, is provided by the Validation Team, and is discussed in [Val Plan]. (These radiances are used by the IFRCC team to establish a vicarious instrument calibration.) Controlling documents for the IFRCC program include the [ISR] and the [FDR], which define the instrument requirements. Included in the reference section are summary publications of the MISR calibration program[1, 3].

Following publication of this plan, the IFRCC team will prepare two algorithm theoretical basis documents. The first, [L1Rad ATB], is a revision to the current [L1B1 ATB], which describes the algorithms used to produce the Level 1B1 Radiometric Product. Processing for this product will occur at the Distributed Active Archive Center (DAAC). The second document is the [IFRCC ATB]. This describes the algorithms which will routinely run at the JPL Science Computing Facility (SCF). In simplified terms, the [IFRCC ATB] describes the instrument calibration process, the [L1Rad ATB] describes the radiance retrieval process.

1.3.1 Controlling project documents

[shorthand]	Reference

- MISR Algorithm Development Plan, JPL D-11220, 11 Apr. 1995.
- MISR Calibration Management Plan, JPL D-7463, 17 Aug. 1990.
- MISR Data Product Description, JPL D-11520, 13 Sept. 1993.

[FDR] MISR Instrument Functional and Design Requirements, JPL D-9988, Rev. A, 29 Nov. 1994.

[ISR] MISR Instrument Science Requirements, JPL D-9090, Rev. B, 25 Aug. 1994.

1.3.2 Reference project documents

[shorthand]	Reference
[GeoCal Plan]	MISR In-flight Geometric Calibration Plan, JPL D-13228.
[IFRCC ATB]	MISR In-flight Radiometric Calibration and Characterization Algorithm Theoretical Basis.
[L1B1 ATB]	MISR Level 1B1 Radiometric Product Algorithm Theoretical Basis, JPL D-11507, Rev. A, 01 Nov. 1994.
[L1Rad ATB]	L1 Radiance Scaling and Conditioning Algorithm Theoretical Basis, JPL D-11507, Rev. B.
[PreCal Plan]	MISR Preflight Calibration Plan, JPL D-11392, 10 Jan. 1994.
[Val Plan]	MISR Science Data Validation Plan, JPL-12626.

1.4 REVISIONS

This is the initial release of this document. The document will be updated annually preceding each new release of the Level 1B1 software.

2. EXPERIMENT OVERVIEW

2.1 MISR SCIENCE OBJECTIVES

The Multi-angle Imaging Spectro-Radiometer (MISR) instrument is part of an Earth Observing System (EOS) payload to be launched in 1998. The purpose of MISR is to study the ecology and climate of the Earth through the acquisition of systematic, global multi-angle imagery in reflected sunlight. MISR will monitor top-of-atmosphere and surface reflectances on a global basis, and will characterize the shortwave radiative properties of aerosols, clouds, and surface scenes. Data from the MISR experiment will enable advances in a number of areas concerning global change:

- Clouds. High resolution bidirectional reflectances will be used in cloud classification, and the spatial and temporal variability of cloud hemispheric reflectance will be determined. Stereoscopic measurements will be used to retrieve cloud-top elevations. These data will help discern the role of different clouds types in the Earth's energy balance.

- Aerosols. Multi-angle radiance data will be used to determine aerosol optical depth, and to identify particle composition and size distribution. These data will enable a global study of the role of aerosols on the energy budget, and will provide data used for surface retrievals.

- Land surface. Retrievals of surface bidirectional and hemispheric reflectances will be used to characterize vegetation canopy structures and for investigating the effect of land surface processes on climate.

- Oceans. MISR will provide data to support ocean biological productivity studies in regions of low phytoplankton pigment concentrations, such as much of the tropical oceans.

2.2 INSTRUMENT DESCRIPTION

The MISR instrument consists of nine pushbroom cameras. It is capable of global coverage every nine days at the equator and 2 days in the polar regions. It flies in a 705-km descending polar orbit and takes about 7 minutes of flight time to observe any given region at all nine view angles. The cameras are arranged with one camera pointing toward the nadir (designated An), one bank of four cameras pointing in the forward direction (designated Af, Bf, Cf, and Df in order of increasing off-nadir angle), and one bank of four cameras pointing in the aftward direction (using the same convention but designated Aa, Ba, Ca, and Da). Images are acquired with nominal view angles, relative to the surface reference ellipsoid, of 0°, 26.1°, 45.6°, 60.0°, and 70.5° for An, Af/ Aa, Bf/ Ba, Cf/ Ca, and Df/ Da, respectively. Each camera uses four Charge-Coupled Device (CCD) line arrays in a single focal plane. The line arrays consist of 1504 photoactive pixels plus 16 light-shielded pixels per array (eight at each end), each 21 x 18 μm is size. In addition, the camera circuitry clocks out 536 overclock pixels. These are samples of the serial register which follow the reading of the active and shield pixel elements. They represent a

measure of the camera offset DN. The instrument electronics capture only the active, last eight shield, and first eight overclock pixels for transmission. Each line array is filtered to provide one of four MISR spectral bands. The spectral band shapes will nominally be gaussian with bandcenters at 443, 555, 670, and 865 nm.

MISR will acquire images in each of its channels with spatial sampling ranging from 275 m (250 m cross-track in the nadir) to 1.1 km (1.0 km cross-track in the nadir), depending on the on-board pixel averaging mode used prior to transmission of the data. The instrument is capable of buffering the data to provide 4 sample x 4 line, or 1 sample x 4 line averages, in addition to the mode in which pixels are sent with no averaging. The averaging capability is individually selectable within each of the 36 channels (nine cameras, four bands each).

2.3 SCIENCE MODES

There are several observational science modes of the MISR instrument.

Global Mode refers to continuous operation with no limitation on swath length. Global coverage in a particular spectral band of one camera is provided by operating the corresponding signal chain continuously in a selected resolution mode. Any choice of averaging modes among the nine cameras that is consistent with the instrument power and data rate allocation is suitable for Global Mode.

Local Mode provides high resolution images in all 4 bands of all 9 cameras for selected Earth targets. This is accomplished by inhibiting pixel averaging in all bands of each of the cameras in sequence, one at a time, beginning with the first camera to acquire the target and ending with the last camera to view the target. The instrument geometry limits the downtrack length of Local Mode targets to about 300 km.

In each of the four *Calibration Modes* the flight photodiodes are turned on. In *Cal-Diode* the photodiodes are turned for one minute during Global Mode and collect Earth data simultaneously with the cameras. In *Cal-Dark* the photodiodes and cameras collect data over the dark Earth in order to monitor dark current noise stability. In *Cal-North* and *Cal-South Modes* the on-board diffuse panels are deployed, and calibration data are acquired for the cameras. Only the Cal-Dark, Cal-North, and Cal-South mode are part of the routine survey. For these, observations are made during a monthly calibration exercise, or more frequently during initial on-orbit testing. Each of these modes clocks through all integration times and camera averaging modes. For this reason these modes will be utilized heavily during instrument functional testing, both preflight and on-orbit.

Calibration data will be obtained for each spatial sampling mode by cycling each channel through the various modes during the calibration period. The latter three Calibration Modes will be used on a monthly basis during routine mission operations, although early in the mission it will be used more frequently.

In addition to these modes, the instrument is commanded into a *Dark Mode* over the dark Earth side of each orbit (excluding Cal-Dark). Here the camera electronics are powered off to conserve energy and there is no data acquisition.

2.4 MISSION OPERATIONS

MISR operates continuously on the dayside of each orbit. Instrument activities are preplanned and scheduled. MISR flight computer commands necessary to carry out the mission objectives are contained in tables covering a 16 day (233 orbit) cycle, which are uplinked on a regular schedule.The instrument commands are loaded by the EOS Operations Center during EOS-AM/Tracking and Data Relay Satellite System (TDRSS) contact periods. During a nominal 24 hour period the instrument cycles between the data acquisition modes and the dark mode on each orbit. Regular calibrations of the instrument are conducted at specified intervals to maintain the integrity of performance. Local Mode observations and data acquisitions will change to account for seasonal effects or for specific activity monitoring.

For each orbit, the beginning orbit boundary is assumed to be the dark side equator crossing (ascending node). This enables all data within a swath, including calibrations, to be planned, commanded, and acquired as a unit.

The four science modes (Global, Local, Calibration and Dark) are within the Spacecraft Science Mode and are not individually commanded by the spacecraft. Other operating modes (Standby, Safe, Survival, Test and Off) have a one-to-one relationship to Spacecraft Modes and can be commanded individually by the spacecraft or ground.

2.5 DATA PRODUCTS

The MISR Science Computing Facility (SCF) and Distributed Active Archive Center (DAAC) are the sites where the functions of MISR data product algorithm development and standard data product generation will be implemented, respectively. The SCF is the site where quality assessment, algorithm and data product validation, and software development occurs. The MISR DAAC, which is shared with several other EOS instruments, is the facility at which software incorporating MISR science algorithms will operate in a high volume, real-time mode to produce standard science data products.

The generation of science data products can be divided into six subsystems within the Product Generation System (PGS). Each subsystem has at least one primary output product, but may have other secondary output products. It is convenient to conceptualize the processes within these subsystems as occurring in sequence, with the predecessor producing at least one complete product, a portion of which is the primary input for the successor. Each of these subsystems correspond to a processing level of a product generation flow, as shown in Figure 2.1. These levels conform generally to the EOS scheme from Level 1 to Level 4. The first two items within the Level 1B process box (radiance scaling and radiance conditioning) are developed under this plan and constitute Level 1B1.

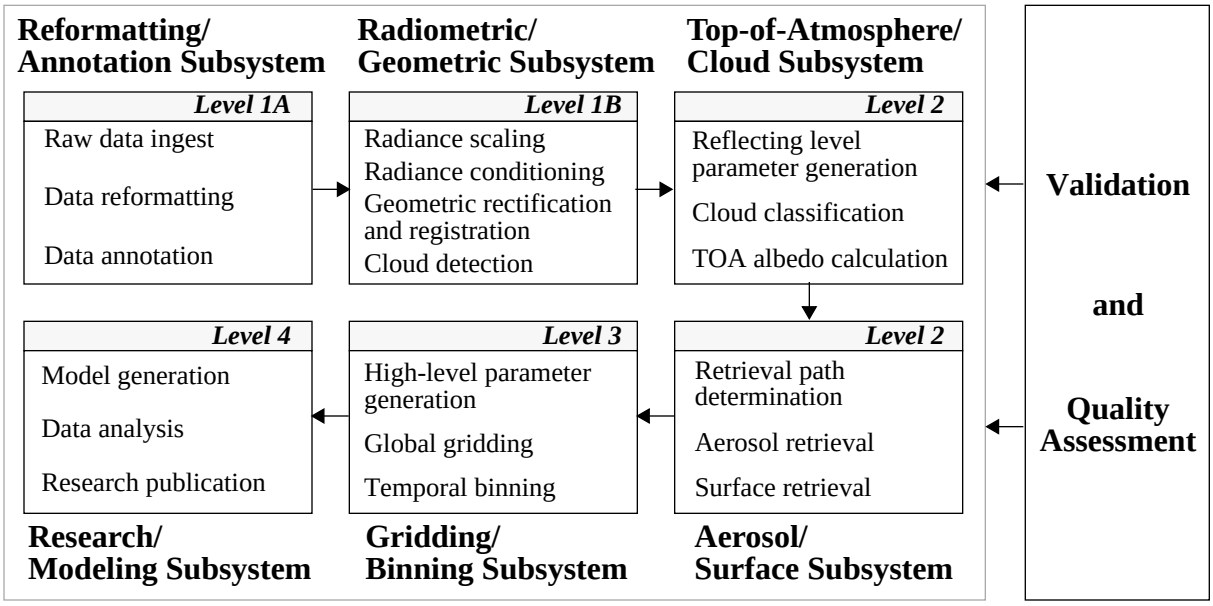

Figure 2.1. MISR Product Generation System

Standard products generated at the DAAC are critically dependent on calibration parameters and other lookup data, such as threshold datasets, atmospheric climatologies, aerosol and surface model datasets, which are produced at the SCF. Functions performed at the SCF are separated from DAAC activities because they require much closer scrutiny and involvement by the MISR Science Team than the MISR DAAC could provide. Updates to these data structures occur infrequently compared to the rate of standard product generation, and therefore fit into the more limited processing capabilities of the SCF. The Level 1A and 1B products are detailed below, as they are most pertinent to this document.

2.5.1 Level 1A Reformatted Annotated Product

Square-root encoding is performed in-flight in order to compress MISR data prior to transmission. Thus, the 14-bit data which are produced by each camera are square-root encoded, through use of a table look-up process, and reduced to 12-bit numbers. At the lowest archive level for MISR data, Level 1A, this step is reversed, then padded to a 16-bit word. That is, the Level 1A data are representative of the original camera output. In addition to these camera DN values, the Level 1A product is appended with platform navigation and MISR engineering parameters, and points to the associated radiometric calibration coefficients, as shown in Table 2.1. Metadata files are generated which assess the data quality by flagging lines of data that are missing, contain one or more saturated pixels, have extremely high average DN values for the array, have DN values for an active pixel which are less than the offset video, or transition from a scene of high reflectance across most of the array, to a scene of low reflectance across most of the array. These conditions may affect the data quality, to some degree, as is discussed in Section 4.2.

Table 2.1. Level 1A product

Product	Principal contents
Level 1A: Reformatted Annotated Product	• Data numbers linearized via square-root decoding • Navigation and engineering data, and pointer to the relevant ARP file.

2.5.2 Level 1B1 Radiometric Product

The Level 1A data are used as input to the Level 1B1 processing code. The primary objective of the MISR Level 1B1 processing algorithm is to produce a measure of incident radiances, averaged over the in-band response profile, from the camera digital numbers (DN). This parameters are summarized in Table 2.2. The radiometric data are reported at the same spatial resolution as the input DN, and no re-sampling is performed. Processing is done routinely on all transmitted MISR data.

Table 2.2. Level 1B1 Radiometric Product

Parameter name	Units	Horizontal Sampling (Coverage)	Comments
Radiance	$W\ m^{-2}\ \mu m^{-1}\ sr^{-1}$	250 m nadir, 275 m off-nadir, or averages per the camera configuration (Global)	• Radiometrically-scaled data • No geometric resampling • 9 cameras, 4 bands • Uncertainty reported in Ancillary Radiometric Product

The algorithm used to produce the Level 1B1 Radiometric Product requires knowledge of the radiometric calibration coefficients for each pixel. This instrument calibration is updated monthly using On-Board Calibrator (OBC) data, vicarious calibration (VC) data, histogram equalization (HE) data, and trend data, as available. The coefficients used in the Radiometric Product generation are documented in the Ancillary Radiometric Product (ARP), summarized in Table 2.4. Also included in the ARP are absolute and relative radiance uncertainties, signal-to-noise (SNR) ratios, spectral parameters, instantaneous fields-of-view (IFOV) information, and various threshold parameters used in Level 1A metadata reports which describe the data quality. The ARP is generated at the MISR SCF, updated as needed, and delivered to the DAAC. Thus, production of the ARP is not part of the routine DAAC processing of MISR data, however it falls within the purview of this plan.

Traditionally, the radiance retrieval is produced using a simple radiance scaling algorithm in which a gain and offset coefficient (specific to each pixel) are used in conjunction with a linear calibration equation. For MISR, a quasi-linear calibration equation that includes a small quadratic term is utilized. In addition, point-spread function deconvolution, and in-band response non-

uniformity corrections are to be implemented. The rationale for these is discussed in Section 4.2. The IFRCC team will also develop an out-of-band correction algorithm, although this processing will occur at higher processing levels.

2.5.3 Ancillary Radiometric Product

The contents of the MISR Ancillary Radiometric Product (ARP) are given in below, in Tables 2.4 and 2.4.

Table 2.3. Level 1B1 Ancillary Radiometric Product: Updated parameters

Updated parameters	Units	Comments
Date range	none	• Revision number • Date/ time range of applicability
Radiometric calibration coefficients	DN/ (W m^{-2} μm^{-1} sr^{-1})$^{-2}$ (G2); DN/ (W m^{-2} μm^{-1} sr^{-1}) (G1); DN (G0)	• 3 coefficients for 1504 pixel values for 9 cameras and 4 bands
Absolute and relative camera calibration uncertainties	%	•Absolute: 1504 pixel values for 9 cameras, 4 bands at 5 radiometric levels • Pixel relative: 1 value per band • Camera relative: 1 value per camera
Signal-to-noise ratios	none	• Values for 9 cameras, 4 bands at 5 radiometric levels for each averaging mode
Data quality indicator	none	• Values: 2 (within specification), 1 (reduced quality), 0 (dead pixel). Provided for each averaging mode.
Level 1A quality assessment threshold parameters	DN	threshold values for flagging lines of data that have • one or more saturated pixels; • extremely high average DN values for the array; • DN values for one or more active pixels which are less than the offset video value for the line; or • transition from a scene of high reflectance across most of the array, to a scene of low reflectance across most of the array.

Table 2.4. Level 1B1 Ancillary Radiometric Product: Static Parameters

Static parameters	Units	Comments
Spectral band parameters (center wavelength, bandwidth, transmittance)	nm	• Equivalent square-band and Gaussian representation provided for each pixel, as well as a typical spectral response profile for each line array.
Spectral in-band nonuniformity correction factors.	none	• Provided for each line array as a function of field-angle.
Spectral out-of-band correction matrix.		• Provides out-of-band correction terms at MISR wavelengths. • Provided for each line array. • Field-angle independent.
Point-spread-functions (PSF)	none	• Unique for each line array.
Instantaneous field-of-view (IFOV)	μrad	• Crosstrack and along track half-power points of pixel responsivity function with angle
Exo-atmospheric spectral solar irradiances	$W\ m^{-2}\ \mu m^{-1}$	• Weighted over each MISR spectral band
PAR integration weights	none	• Used at Level 2 for generation of albedos in photosynthetically active radiation (PAR) region.

2.5.4 Metadata

The MISR Level 1B1 Radiometric Product will contain metadata. These support cataloging and searching of the data and provide additional data quality assessment flags. The specific contents of this file will be developed as part of the Level 1B1 algorithm development effort.

3. CALIBRATION OVERVIEW

3.1 REQUIREMENTS

The only directly measured physical parameters observed by MISR are camera incident radiances. All geophysical parameters, such as aerosol optical depth, cloud-fraction bidirectional reflectance factor, or hemispheric reflectance, are derived from these data. Thus, MISR has defined its instrument specification, calibration, characterization, and ground processing requirements to meet the needs of its scientific community. In terms of absolute radiometry, MISR performance is driven by the desire to:

- determine changes in the solar radiation budget, and thus provide data for global climate studies;
- produce a data set of value to long-term monitoring programs and allow intercomparisons of data on time scales exceeding that of an individual satellite; and
- provide EOS synergism, and allow data exchanges between EOS-platform instruments.

Not all of the MISR measurement objectives are dependent upon high accuracy in the absolute radiometric calibration. For example, the determination of the shape of angular reflectance signatures of surfaces and clouds are dependent on the relative camera-to-camera and band-to-band radiometric accuracy. The requirements for relative calibration have therefore been made higher than the absolute requirements, in order to meet the needs of these products.

The requirements derived from the above considerations are challenging, and have been defined in several controlling documents, including the [ISR] and [FDR]. As examples, radiometric accuracy must be within ±3% (1σ) over high reflectance, spatially uniform scenes, and polarization insensitivity is to be better than ±1%. The instrument must be unaffected by image blur and scattering at less than the 2% level for a 5% equivalent reflectance (e.g., ocean) scene 24 pixels distance from a high-contrast edge (e.g., a cloud boundary). All performance requirements must be met through mission life.

3.2 DETECTOR-BASED CALIBRATION

The performance requirements specified for MISR influence both the design and testing programs. MISR has been designed to meet short term stability and long term degradation requirements. Radiation resistant components have been selected, as needed for the planned EOS orbit environment. Sun blockers, lens shades, and a cover will prevent direct Sun illumination of the MISR front optical element. UV illumination, in the presence of surface contamination, might otherwise result in polymerization of the surface constituents and a decrease in optical throughput. The design also minimizes stray light.

MISR radiometric accuracy objectives are met through instrument design and usage of detector-based calibration technology. The latter is utilized at institutions such as the National

Institute of Standards and Technology (NIST) and the National Physical Laboratory of England. Detector-based technology avoids the uncertainties associated with the transfer of scale from one source to another, and more importantly, those associated with lamp instabilities which increase with time. The measure of incident radiance is provided with the standards, through knowledge of their internal quantum efficiency (nearly 100%), filter transmittance, and the baffle tube area-solid angle product.

For the preflight radiometric calibration, off-the-shelf, high quantum efficiency, trapped laboratory standards are utilized. Precision apertures have been added by the MISR test team, to define the fields-of-view for these standards. A verification has been made by evaluating the precision of the radiance measurement among the various standards. Additionally, a round-robin study has been conducted in which the participants sequentially viewed the JPL/ MISR integrating sphere. Agreement was within 1%, thus giving us confidence in our 3% uncertainty estimate[1]. Participating were calibration scientists from the Optical Sciences Center, University of Arizona; National Research Laboratory of Metrology (NRLM), the Japanese standards laboratory; and Goddard Space Flight Center (GSFC). Upon completion of the preflight activities, the standards will be sent to NIST for further verification of the radiometric scale achieved with use of these standards.

The flight instrument contains an On-Board Calibrator (OBC) which likewise makes use of detector standards. The radiance scale for these is determined from a transfer of scale established by the laboratory detector standards, using a small dedicated integrating sphere. The tie between the preflight and in-flight radiometric scale is verified as both the flight and laboratory diodes have an opportunity to view the laboratory integrating sphere. Additionally, the flight diodes are measured for quantum efficiency, filter transmittance, and baffle-tube geometry.

MISR's radiometric scale is traceable to NIST and other EOS sensors through the reporting of radiances in SI units as accomplished with use of the preflight and in-flight detector standards, and verification of the same.

3.3 CALIBRATION EQUATION

Each photoactive pixel element stimulated with incident radiation responds with an output measured in digital numbers (DN). The plot of incident radiance versus DN is termed the radiometric transfer curve. The objective of radiometric calibration is to develop a calibration equation which best represents the observed radiometric transfer curve, and to provide both a quantitative determination of the gain coefficients to this equation, as well as the uncertainties in measuring radiances using these coefficients. Radiometric calibration is best conducted using a full-aperture (one that overfills the sensor's field-of-view), spatially and spectrally homogeneous source. Multiple radiometric levels are used, spanning that portion of the sensor dynamic range that is of interest to the data community. Radiometric uncertainties that arise due to specific scene features (e.g., high contrast targets) are reported as part of the IFRCC characterization program.

Sensor gain is primarily a function of the optics transmittance (having a strong field-angle dependence), the filter transmittance, CCD quantum efficiency, the amplification of the electronics and the analog-to-digital conversion factor. Local deviations in response are due

equally to filter pinholes or scatter sites and CCD site defects. The gains associated with the individual detector elements can change with time, due to polymerization of contaminants, lens browning, and the effects of radiation on the electronics. Because of this anticipated degradation with time, the radiometric response is monitored during the mission.

During preflight calibration it was determined that a quadratic calibration best represents the radiometric transfer curve for each of the cameras. Although the CCD response is nearly linear (the second order coefficient is quite small), inclusion of this term improves the radiance retrieval at the lower end of the detector transfer curve.The equation MISR will use is thus:

$$DN - DN_o = G_o + G_1 L_\lambda + G_2 L_\lambda^2 .$$

where

L_λ is the sensor band-averaged spectral incident radiance, averaged over both in-and-out-of-band wavelengths, reported in units of [W m^{-2} sr^{-1} μm^{-1}], and defined by the equation:

$L_\lambda = \frac{\int L_{source} \Re \lambda d\lambda}{\int \Re \lambda d\lambda}$ and R is the relative instrument spectral response;

DN is the camera output digital number,

G_0, G_1, and G_2 are the response coefficients which, once determined, provide the radiometric calibration of a specific pixel,

DN_o is the DN offset, unique for each line of data, as determined by an average over the first eight "overclock" pixel elements.

It is noted that prior to data transmission, the MISR system electronics square-root encode the camera DN values. This process is inconsequential to the current discussion, as camera output DN data were used directly for the preflight radiometric calibration analysis. Neither will it be of concern for the in-flight regression, as the Level 1A product, used as input to the Level 1B1 processing, restores the original camera DN values.

During preflight calibration, a Fidelity Interval Analysis[4] has been used to estimate the uncertainty in the inverse regression from the fit (that is, the uncertainty in measured radiance for a given DN). Fidelity Interval Analysis has also been used to define the calibration experiment, specifically the number of radiometric levels to be used during calibration, as well as the number of independent data repititions. This tools will continue to find use in the in-flight program, and will be used to estimate uncertainties in the radiances computed by DAAC processing.

3.3.1 Source color

For other instruments programs, source color temperature tables have been provided to correct the preflight coefficients for differences in laboratory blackbody versus solar color temperature. As the MISR ARP coefficients represent the ratio of output DN to total band weighted radiances, there is no need to provide such a correction. (If the processing were to correct for out-of-band differences due to the source color temperature, for a uniform reflectance scene, such a need would exist). MISR will perform out-of-band correction at Level 2, where scene spectral information is available (since the band data are registered at Level 1B2).

3.4 IFRCC OBJECTIVES

The objectives of the IFRCC task are:

- to provide for the in-flight radiometric calibration of the sensor and validate that this calibration meets the absolute and relative accuracy requirements, as defined by the [ISR];

- to deliver this calibration to the DAAC in the form of the Ancillary Radiometric Product (ARP), and update this product as needed to maintain the accuracy of calibration;

- to develop the radiance scaling and conditioning algorithms, used in Level 1B1 standard product generation at the DAAC;

- to provide for the characterization of the sensor, as needed to define the impact of hardware performance on the scientific products; and

- to validate radiances produced from the radiance scaling and conditioning algorithms.

A high-level summary of these activities is given in Figure 3.1. Here, also, the input data types and output products and deliverables are depicted. The IFRCC team will develop SCF algorithms and processing codes to explore MISR performance and provide the needed radiometric calibration and characterization products and reports. Non-MISR input data sets include the vicarious in-situ measurements, used in vicarious calibration processing, and cross-sensor data, used for calibration verification. The development of the Level 1B1 Radiance Product algorithms is primarily a prelaunch activity, with post-launch updates as needed. The calibration, characterization, and calibration integrity activities are on-going processes in the post-launch era.

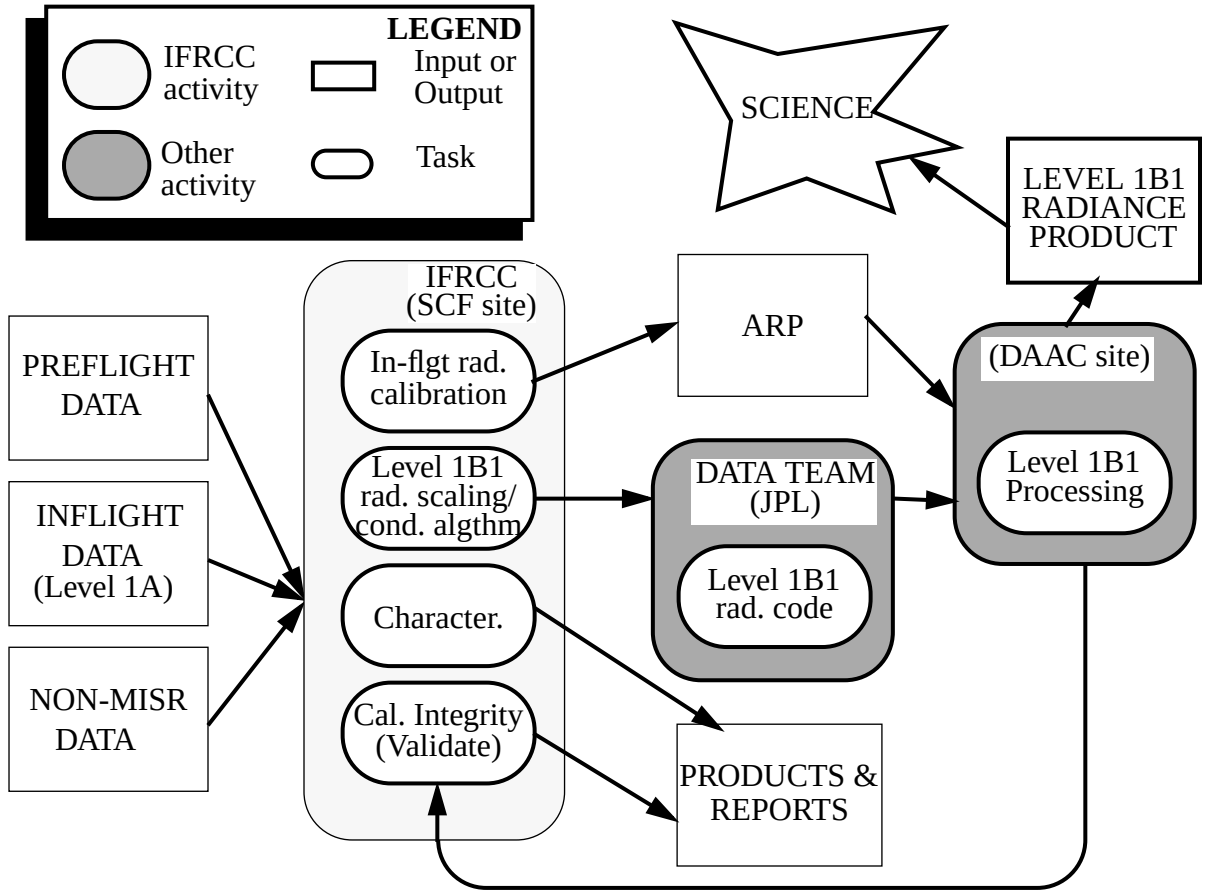

Figure 3.1. IFRCC program elements.

Figure 3.2 shows an expanded view of these IFRCC activities. Post-launch MISR data acquisition is controlled through mission operations and the commanding of the science modes. The IFRCC team receives Level 1A data through the DAAC. Both Calibration Mode and Local Mode data are used, each supporting an independent calibration methodology. In all, four calibration methodologies are weighted to produce the ARP radiometric coefficients and radiance uncertainty tables. These are On-Board Calibrator (OBC), vicarious calibration (VC), histogram equalization (HE), and data trend methodologies. Characterizations will include noise analyses, and radiometric uncertainties as quantified for a variety of specific scenes types (having high spatial or spectral contrast). Finally, calibration integrity and Level 1B1 validation will be accomplished using cross-sensor comparisons and MISR desert scene data. Lunar calibration data will be additionally analyzed for stability verification purposes, if made available. The processing steps depicted in this figure will be described below and in the following chapters.

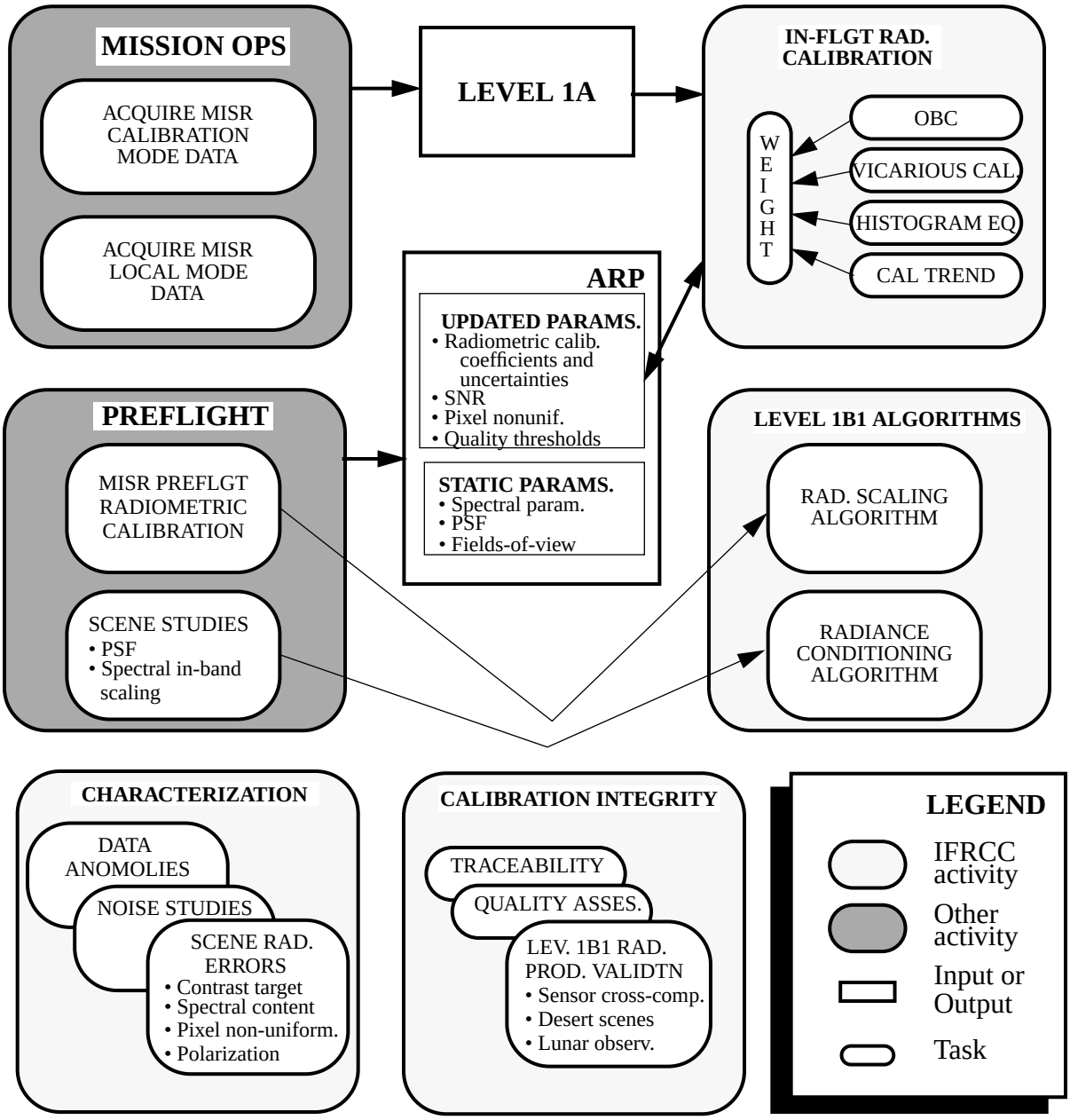

Figure 3.2. IFRCC program element breakdowns.

3.4.1 In-flight radiometric calibration

MISR is routinely calibrated in flight to account for anticipated degradations in sensor response with time. Preflight calibration data are used to establish a prediction of the initial on-orbit response. These data have less influence with time, as the trend is established with more and more on-orbit measurements. For the preflight, OBC, and VC methodologies, spatially and spectrally featureless targets are used to establish the calibration response.

Multiple methodologies are utilized in the in-flight program in order to reduce systematic errors and to provide a measure of calibration accuracies. The OBC provides frequent time sampling (monthly) of the instrument radiometric response. These data will be indispensable in the verification of sensor response stability following undesirable spacecraft events (if they should occur), such as a maneuver which may cause sunlight to fall on the front-surface optical elements. In using these data, however, it must be verified that there are no differences in measured response than that which would be obtained in viewing an Earth-target. As a general rule, the most accurate calibrations are obtained with the sensor operating under the same conditions as during science data acquisition. This is not the case when the cameras view the diffuse panels, irrespective of how well the design specifications have been met. Stray light and front surface reflections between the MISR camera and calibration panel have the potential of introducing an error source in the calibration. By including other methodologies in the analysis, any such systematic bias is detected.

The VC data require good weather conditions, and involve a staff and instrument team which must be transported long distances to suitable test sites. Aircraft underflights, although potentially providing the most accurate calibrations, are typically limited due to cost considerations. Coordination among other sensor teams is also required. For these reasons VC campaigns are less frequent than the OBC experiments. Semi-annual VC campaigns are planned. Because vicarious experiments are less controlled (with unpredictable weather), clearly these measurements are not a substitute for the OBC data. Rather, the data sets complement each other.

HE utilizes Earth scene data to make slight adjustments to the response coefficients. This is done to remove striping that might otherwise be present in the radiance product. These data are used to refine the relative calibration of the pixels within each camera, but is not a substitute for the absolute response determinations of the OBC and VC observations.

Trending of the data is an important element of the calibration program. By consideration of previous calibration determinations, abrupt changes in sensor reported response is avoided. Without this element, variations from one reporting to the next would cause erroneous fluctuations in the retrieved radiances. It is believed that any real change of the instrument response will be slowly varying with time (in the absence of a spacecraft event which results in direct solar illumination of the optical surfaces, or which creates significant contamination).

Response coefficients produced from these four methodologies are combined to generate a single representation of sensor response. The coefficients are used to update the ARP, which is then delivered to the DAAC and used in any subsequent processing. The ARP is planned to be updated monthly.

3.4.2 Level 1B1 Radiometric Product algorithm development

Sensor calibration data are used in the production of the MISR standard radiance product, termed the Level 1B1 Radiometric Product. Although processing occurs at the DAAC, it is the responsibility of the IFRCC team to provide the algorithms, which the MISR Science Data System Team turns into production software. The algorithms are broken down into two types. In the radiance scaling processing step, digital number (DN) values are converted to band-weighted

spectral radiances. The second process is termed radiance conditioning. Here, the radiances are adjusted to spectrally scale the measured radiance, predicting the value measured by a nominal passband. In addition, image sharpening is performed using PSF data. Out-of-band spectral response subtraction is performed on select Level 2 products.

For this processing, the Level 1B1 and Level 2 processing algorithms require calibration data sets. Several parameters are available only through the preflight test and analysis program. Examples are the spectral calibration and point-spread function parameters. These parameters are treated as static, as they are believed to be temporally invariant, although on-orbit characterizations will be done to test these assumptions.

The radiometric calibration data will be updated throughout the mission. This is accomplished through the delivery of a new ARP file. Monthly updates are planned, or as needed to maintain an accurate record of the instrument performance. The ARP also provides an estimate of radiance uncertainty (assuming a uniform scene) at several radiometric levels.

The calibration data used in Level 1B1 processing are summarized in Table 3.1. Algorithm development will proceed with the preflight data. In addition to these corrections, MISR Level 2 processing will remove any spectrally out-of-band contribution to the reported radiance, as deemed necessary for that product. Calibration data used for this Level 2 correction is additionally reported in the ARP.

Table 3.1. Calibration data sets

Processing step	Processing level	Required calibration data	Comment
Radiance scaling	Level 1B1	Radiometric gain coefficients	Preflight, updated monthly in-flight
Radiance conditioning	Level 1B1	Spectral in-band parameters	Preflight, static
	Level 1B1	Point-spread function response	Preflight, static
	Level 2 (selected products)	Out-of-band response subtraction	Preflight, static

3.4.3 Characterization

Characterization is the measurement of the typical behavior of instrument properties which may affect the accuracy or quality of the derived data products. The in-flight characterization includes a determination of the noise and spatial frequency response of the sensor. It determines the potential for radiometric errors as may occur for specific scene types, including those of high spatial or spectral contrast. Finally, the in-flight characterization program will attempt to confirm that many instrument properties are as measured in the prelaunch

laboratory environment. This includes spectral response stability, hysteresis, saturation recovery, and modulation transfer function (MTF).

3.4.4 Calibration integrity

Calibration integrity is the process of validating and certifying the Level 1B1 Radiometric Product. One component of calibration integrity is determination of any radiometric biases between the MISR radiometric scale, and that used by other remote sensing instrument (particularly EOS sensors). Periodic cross-comparisons with Moderate Resolution Imaging Spectroradiometer (MODIS), Système Probatoire d'Observation de la Terre (SPOT), and Landsat Thematic Mapper (TM) sensor calibrations will be made, as data are made available. As an added check on the radiometric calibration, there will be a routine analysis of MISR imagery over desert sites. Likewise, response stability may be verified using lunar observation data, if available.

Quality assessment and traceability of the radiance scale are also tasks that will be performed within this program.

4. PREFLIGHT CALIBRATION AND CHARACTERIZATION

The IFRCC program elements are dependent on the preflight calibration, characterization, and verification data products. It is through these preflight reports that the need for radiance conditioning, as an element to the Level 1B1 Radiometric Product processing, has been identified. Further, the Level 1B1 algorithms, as delivered for initial processing of MISR post-launch data sets, will be developed using the preflight data sets.

The purpose of the preflight program is to:

- verify that instrument design conforms to specifications;
- establish as-built performance;
- test for sensor response anomalies;
- provide an at-launch estimate of the sensor's radiometric calibration; and
- provide those calibration data sets which would otherwise be unobtainable in flight, including the spectral and PSF parameters.

4.1 PERFORMANCE TESTING OVERVIEW

Details of the preflight calibration program are provided in [PreCal Plan]. A brief overview is provided here. Some degree of testing of MISR flight hardware is done at the component, camera, and system levels, as well as after shipment and integration onto the spacecraft. The bulk of the science performance data, however, are collected at the camera level of assembly[1]. By characterizing each camera individually, testing can be spread over time and the test hardware is simplified. Camera testing is done using two MISR-dedicated thermal vacuum chambers. The shorter system level tests are conducted in shared, more costly facilities.

After assembly a camera first goes to the Optical Characterization Chamber (OCC). A xenon lamp source external to this chamber feeds a chamber-internal target wheel. At the target wheel a pinhole is selected according to the focal length of the camera under test. The pinhole target is at the focus of a collimator, allowing the camera to image the pinhole which produces a subpixel Airy disk when well focused. As the camera is attached to a two-axis gimbal, this pinhole image can be scanned across the focal plane in either the downtrack or crosstrack directions. With this set-up the OCC is used to provide the boresight, MTF, point-spread-function (PSF), effective-focal-length, and distortion mapping of the sensor.

Following completion of OCC testing, a given camera is moved to the Radiometric Characterization Chamber (RCC). This chamber has a window within its door. Either a monochromator or integrating sphere are wheeled in front of the chamber, illuminating the camera through this window. Radiometric and spectral calibration camera data are acquired while in this chamber.

In-band spectral calibration data are taken at five field-angle locations across the array; out-of-band calibration data are taken at three field-angle locations. (The monochromator exit beam is too small to illuminate all but a few pixels simultaneously. It is possible to slew this beam into many camera field angles, but the length of time required to scan through all wavelengths limits the number of field positions tested.) Out-of-band response beyond the limits of the monochromator (less than 400 or greater than 900 nm) is determined by using the measured focal plane spectral response data (CCD, filter, and window), collected to 1000 nm, and a lens transmittance model. The spectral response of the MISR cameras are known to be limited to above 365 nm, due to lens transmittance, and below 1100 nm, due to the bandgap of the silicon detectors.

The out-of-band spectral calibration data are verified by a test which uses the laboratory integrating sphere and a set of Rugate filters. The filters are notched in spectral transmittance, and pass light only at MISR out-of-band wavelengths. There are four Rugate filters, one for each MISR band. They provide a measure of the total, integrated out-of-band response, and do so for every pixel. The Rugate filters were procured after camera calibration data began, and were therefore used in the testing of most, but not all, of the cameras. Although the Rugate filter data are valuable, the monochromator data are used to provide the out-of-band spectral calibration. These give the spectral response shape, and are available on every camera.

Radiometric stability is verified at the system level of assembly by deploying and illuminating the flight diffuse panels. The illumination system for this test is called the MISR Aliveness and Stability Test (MAST). Instrument geometric stability is characterized at the system level with use of a calibrated nine-collimator fixture which rests on the instrument optical bench during test. This fixture is called the Collimator Array Tool (CAT).

The preflight program provides for the reflectance characterization of the flight OBC diffuse panels. Data are acquired at three laser wavelengths (442, 632.8, and 860 nm). Principal-plane reflectance data have been acquired for three angles of illumination and through a range of view angles. This is done for all Flight and Engineering Model panels. Reflectance data at other view azimuth angles, and for two states of input polarization, have been acquired on smaller test pieces. The test pieces were fabricated and machined simultaneously with the flight hardware. For these measurements, angular sampling is sufficient to provide a measure of hemispheric reflectance, once the data are integrated over angle. Test-piece data are used to construct the bi-directional reflectance function (BRF) for the flight units. The BRF data base is used by the OBC calibration algorithm, which provides a measure of the post-launch radiometric calibration of the cameras. They are used to transfer the measure the photodiode incident radiances to camera incident radiances. Verification of the BRF data is provided from the hemispheric reflectance computation, as compared to the vendor provided value. Additionally, verification of the identity of test piece and flight unit reflectance properties has been accomplished by comparing principal-plane data acquired for each of these.

Flight photodiode radiometric responses are determined from use of a small integrating sphere, calibrated using the laboratory photodiode standards. Data from both a component analysis and system testing (viewing the large integrating sphere used to calibrate the cameras, and spectral response determination) have also been acquired. The component response

determination was originally planned for the flight HQE devices, as higher accuracies are obtained if the devices can characterized from fundamental physics, rather than from a transfer response using another standard. However, the flight photodiodes are known to be subject to an out-of-band response, not characterized by the Cary filter transmittance data. The laboratory standards have negligible out-of-band response.

4.2 CAMERA PERFORMANCE SUMMARY

Detailed analyses of preflight camera data from the OCC and RCC have demonstrated:

- signal-to-noise ratios are met with considerable margin, operating with photon limited noise performance over much of the dynamic range, and dark current contributing only a few DN of noise at temperature;
- the Lyot depolarizer is effective in scrambling the incoming polarization state, making the cameras radiometrically insensitive to the incoming state of polarization;
- MTF and focus requirements have been met;
- spectral response knowledge requirements have been met; and
- the radiometric accuracy requirements have been met.

The following unexpected performance characteristics have been noted, however, which impact the ground processing plans:

- there are typically a half dozen pixels per array that have deviations in response of about 10% lower than their neighbors, due to filter pinholes or other minor defects;
- focal plane scatter can be evident 30 pixels distance from the geometric image point, causing a low-level halo;
- center wavelengths can vary in uniformity by a half nanometer across an array, or by several nanometers from one camera to another;
- the integrated out-of-band response can be as large as 3% of the in-band signal;
- the offset DN is a dynamic parameter that depends on average array illumination, illumination history, and spectral band;
- the response of the adjacent pixel can be anomalous, when a given pixel is illuminated over its channel stop under conditions of sub-pixel illumination; and
- that saturated pixels may affect the DN of neighboring non-saturated pixels.

These performance variables are summarized in the discussion which follows. It is one objective of the in-flight program to make use of these data and provide ground processing corrections to the data, as needed to meet the [ISR] requirements.

4.2.1 Pixel nonuniformity of response

Problem: Pixel uniformity of response is compared to the average response for each four-pixel set across the array. It has been found that there are typically a half-dozen pixels sets which exceed the requirement that each pixel in the set have no more than a ±3% (1σ) deviation from the mean. If 4x4 on-board averaging is selected, radiometric errors can result for these pixels if the scene radiance is also non-uniform across the four pixels. The magnitude of the error is scene dependent, and increases in proportion to scene inhomogenity.

Cause: This camera feature results from local filter spatter sites and pinholes, as well as local CCD defect sites. The contributions seem to be equally distributed between the filter and CCD.

Impact on the Level 1B1 algorithm: No correction for this effect is presently planned for standard data processing, as the affected data is a small fraction of the whole. The afflicted four-pixel sets will, however, be flagged via the ARP Data Quality Indicator, alerting higher level processing to potentially poorer radiometric accuracy for these averaged pixels.

4.2.2 Low-level halo

Problem: There exists a low-level halo in the camera PSF. This extends for a distance of about 30 pixels to either side of the image, and decreases in intensity with distance. The magnitude of the halo, in the worst case, is no larger than 0.1% of the PSF peak. However, its presence results in violation of one contrast target specification, given in the [ISR], regarding radiometric accuracy of dark fields surrounded by a bright expanse.

Cause: This finite PSF results from scattering of light between the CCD and filter[2].

Impact on the Level 1B1 algorithm: A deconvolution routine will be implemented using PSF data collected during preflight testing. Without the deconvolution there is a 15% radiometric error for the "lake" scene identified in the [ISR]. The deconvolution routine reduces the error such that the 2% contrast target specification is met.

4.2.3 Spectral in-band variability

Problem: The line arrays and cameras have varying center wavelength and bandwidth parameters. The Gaussian results (an analysis of the in-band response) show variations in center wavelength of as much as 3 nm. This feature is undesirable in that the science data product retrievals assume that a single wavelength characterizes each band in all cameras, regardless of field position.

Cause: The filters are non uniform in spectral throughput, as limited by the deposition process.

Impact on the Level 1B1 algorithm: The radiances will be adjusted to a nominal in-band spectral response profile.

4.2.4 Spectral out-of-band response

Problem: Cameras exhibit an integrated out-of-band response as large as 3% of the integrated in-band spectrally response. This is three times larger than the camera specification allows.

Cause: Spatter sites on the filter are believed to redirect light at large angles. As the blocker coatings were not designed to be effective under these illumination conditions, the cameras suffer from a larger out-of-band rejection than predicted from filter-only transmittance measurements, which do not record the scattered light. Pinholes in the filters also contribute to white-light leakage.

Impact on the Level 1B1 algorithm: Correction requires spatial registration of the spectral bands, which is not available at Level 1B1. Thus, spectral calibration data will be generated and stored as static correction coefficients in the ARP, and used to compensate for that portion of the signal contributed by the out-of-band response. This processing is done for select Level 2 products.

4.2.5 DN offset

Problem: The DN offset for the cameras is a dynamic signal. It is unique to each of the 36 channels, and is proportional to the average illumination across the array. It is the result of signals from the video offset voltage circuitry, baseline stabilization circuitry, and detector leakage and dark currents. When the incident signal changes in time from one state to another, it takes about 25 line repeat times for the offset signal to adjust to a new steady-state value. The difficulties associated with this variable offset are:

- The eight shielded pixels at each end of the CCD line arrays do not adequately measure the offset DN. Light leaks make these pixels ill-suited to this purpose. The instrument will therefore be configured to output overclock pixels. (The overclock pixels are produced by sampling the serial register after all the active pixels elements have been read out). The overclock signal provides a direct measure of the DN offset, for every line of data.

- The overclock signal is sampled by the camera electronics to create a baseline stabilization (BLS) signal that is one component of the DN offset. The purpose of BLS is to insure there is no data loss due to an offset DN signal which is set too small. It is believed that the electronics can change quickly, if exposed to a harsh radiation environment. For this reason a fixed, but selectable, offset was not chosen for the design. However, since there is a time constant associated with the BLS, the temporal

response of the DN offset can create situations where there is a loss of data. For example, in going from a view of a full-field bright target (cloud) to a dark target (ocean), the DN offset may momentarily be greater than the DN signal associated with the ocean target. An undershoot off-scale reading has been noted for as many as three line times in simulating this scenario. Actual on-orbit occurrences of this type are expected to be rare.

- There exists a spatial dependence of the offset DN across the array. This may exist due to an overflow of electrons from the serial register into trapping sites, when the illumination is near full scale. The trapped charge migrates back into the serial register with time, once the charge in this register is reduced, then contaminates the active pixel readings. It is estimated that in the worst case (near-IR band), an offset error of 25 DN or less will be produced. Although there is no way to monitor and subtract this noise signal, this error is too small to lead to a violation of the radiometric accuracy requirements. Under consideration, however, is a proposal to reduce this uncertainty even further by reducing camera integration time. This is effective as less of the sensor's dynamic range is utilized, and charge overflow situations are avoided. It would have, if implemented, the adverse consequence of somewhat reducing signal-to-noise.

Cause: The offset DN signal results from a complex interaction of the video signal, baseline subtraction, dark current, and leakage currents.

Impact on the Level 1B1 algorithm: The DN offset will be measured by an average of the first eight overclock pixels and subtracted from the active pixel DN as part of the radiance scaling algorithm. This represents the actual DN offset to a sufficient degree of accuracy. A complete error analysis will be provided by the preflight characterization team.

4.2.6 Saturation

Problem: Pixel saturation occurs when the illumination signal is larger than the available DN range of the detector. A data loss occurs when the maximum DN value is recorded, as there is no way to retrieve a measure of the signal. The maximum radiance which can be measured varies across the array, due to field-angle dependent transmission differences.

Preflight testing has demonstrated that when a pixel is saturated, there is a contamination of neighboring pixels. The neighboring pixels have a DN value which exceeds that predicted from knowledge of the input radiance. This radiometric error decreases with distance from the saturated pixel. The effect appears to be present only in pixels clocked out after the saturated pixel.

Cause: Due to the unsymmetrical nature of the observation, it is believed to be caused by the camera signal chain electronics.

Impact on the Level 1B1 algorithm: There will be a radiometric error in pixels clocked out following the saturated pixel. This error decreases with distance from a saturated pixel. The width

is the affected area is about 30 pixels. Data Quality Indicators within the Level 1A product will flag this condition.

4.2.7 Sub-pixel illumination

Problem: During crosstrack scanning of a subpixel spot across the array, there have been cases reported where the DN of the adjacent pixel decreases as the image approaches the pixel. As the signal is know to increase for this case, the data clearly misrepresent to scene. This situation seems to occur when there is illumination of the channel-stop, however the magnitude of the error seems to be camera and band dependent.

Cause: The cause of this phenomena has yet to be determined. It is clearly electrical in nature, as no optical absorption or scattering mechanism can account for the observation.

Impact on the Level 1B1 algorithm: It is rare that an actual scene will illuminate the array in this manner, where a large signal falls on the channel stop, and little energy falls on the active pixel element. In the event a DN value less than the offset for that line is recorded, a data quality indicator will report the problem.

4.3 ARCHIVAL OF PREFLIGHT INSTRUMENT DATA

The preflight camera reports and calibrations are maintained in both hardcopy and electronic form. Reports include:

- pinhole response (providing verification of focus, stray-light, hysteresis, and point-source-function (PSF) determination);
- radiometric calibration (providing response coefficients, signal-to-noise verification, pixel uniformity of response, and short-term stability)
- spectral calibration (including out-of-band response);
- polarization verification;
- radiometric model (including the nominal flight integration time).

This electronic archive provides a traceable path to the camera verification, characterization, and calibration data sets. An algorithm description, data analysis procedure, and uncertainty analysis will also be provided for each test.

4.4 SPACECRAFT INTEGRATION

4.4.1 Calibration panel exchange

During testing of the calibration diffuse panels it was determined that the spatial uniformity of the Flight panels was superior to that of the Engineering Model units. Further,

during flight qualification of the panels[5,7], the predicted degradation was determined to be a function of contaminants. For this reason it was decided to initially install the Engineering Model panels onto the instrument. Following all observatory level testing, the Flight panels will be installed, replacing the Engineering Model units. Proper orientation of the panels is crucial, as the panels do not have a symmetric bidirectional reflectance function (BRF). It is physically possible to install the panels in the wrong left/ right orientation, as compared to that assumed by the BRF data base.

4.4.2 Degradation check

Degradation testing will be done in ambient pressure and temperature conditions at several points in time during observatory-level instrument integration. This includes post-ship from JPL, and prior to shipping to the launch site. Testing will utilize the MAST where possible. During thermal-vacuum testing the integrator will provide a simple illumination system to verify functionality and Science Mode operability.

5. IN-FLIGHT RADIOMETRIC CALIBRATION

For the in-flight radiometric calibration, multiple methodologies allow higher calibration accuracies, in that they provide a reduction in systematic errors. The smoothing of the coefficients with time prevents an abrupt reported radiance change for a given radiance scene. MISR will combine four calibration methodologies in order to derive the in-flight radiometric calibration

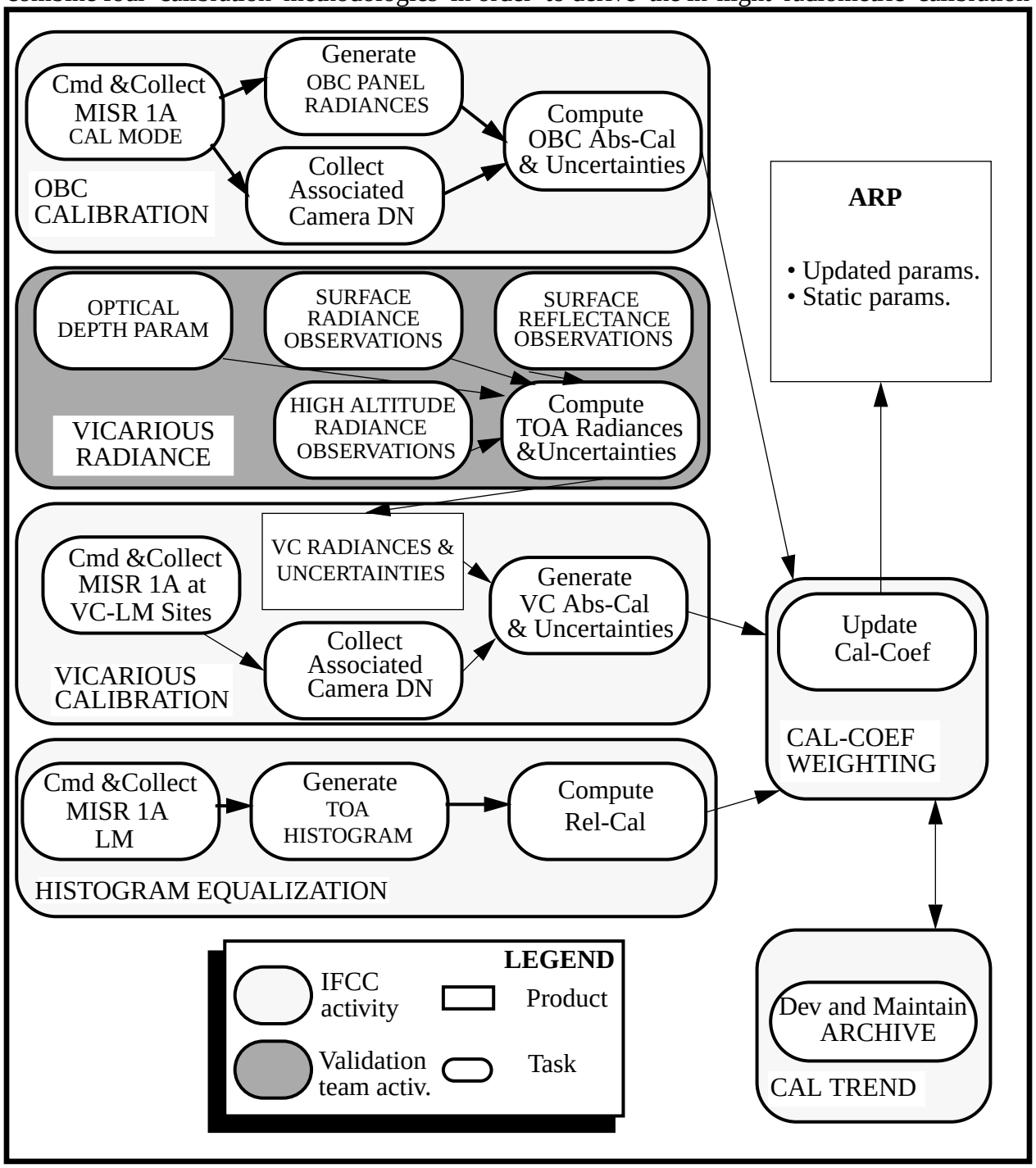

Figure 5.1. Radiometric calibration task.

coefficients. These pathways utilize OBC, vicarious calibration (VC), histogram equalization (HE), and trending data sets, as depicted in Figure 5.1.

It is anticipated that these multiple data sets will not all provide the same radiometric calibration, and that discrepancy conflicts will need to be resolved. Figure 5.2 depicts post launch sensor degradation, as might be measured for the OBC (PIN and HQE detector standards), vicarious, and trend determinations. Histogram equalization is not shown in this figure, as it provides relative-pixel response, rather than long-term degradation information. The trend data are the retrospective coefficients, including the preflight data. For each of these methodologies an uncertainty analysis, the frequency of data collection, and overall data quality metrics will be utilized to define a weighing coefficient. These weighting coefficients may be reassigned with time. Following the weighting of the various methodologies, a single coefficient set is computed, and delivered to the DAAC for subsequent processing of MISR data. This coefficient set is used until updated by subsequent calibrations. That is, the most recently measured (as distinct from the predicted) calibration parameters are used in radiance retrieval. Note that if only the preflight calibration parameters were used, the radiance error would grow with time, as no compensation for sensor degradation would be made. MISR specifications allow for a 10% mission life degradation in sensor response [ISR]. It is believed that signal-to-noise and dynamic range requirements will be maintained, provided the sensor maintains this budget.

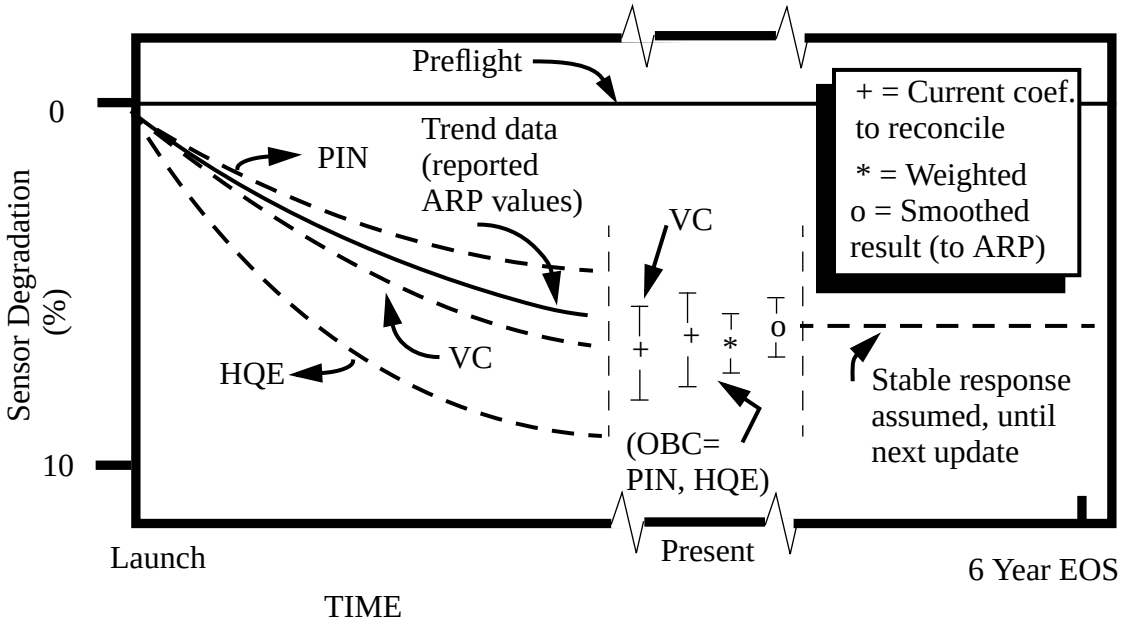

Figure 5.2. MISR degradation, as measured by multiple methodologies.

The preflight coefficients have more of an impact on the ARP in the early months of the mission, when on-orbit data are scarce. They are folded in via the calibration trend history. With time they have diminishing influence on the sensor in-flight calibration. Radiance, as determined using the HQE photodiode standards are also weighted less with time. Their stability has been measured preflight, and used to develop an uncertainty model which grows with time. Currently the plan is to weight HQE and PIN photodiode data equally for the first six months of flight, after which the HQE may degrade in known quantum efficiency. The HQE and PIN flight photodiode

response functions will be verified by analysis of Earth-view data (the photodiodes may be turned on during Cal-diode data acquisition). Any change in response will result in that hardware element having less influence on the camera calibration.

Figure 5.3 summarizes the calibration coefficient weighting processes. The OBC data are utilized to deduce a degradation scale factor for each channel (detector array). This is weighted with the most recent vicarious calibration, to predict the current degradation, as compared to the initial on-orbit response value. The new scale factor is added to the table of the past values, and used to derive an expression of degradation with time. The final value is derived from this expression, evaluated for the present time. This process smooths the reports, and removes any high frequency instability in the values. The resulting scale factor multiplies the current relative calibration function for the array, to produce the reported ARP values. An exception to this smoothing process might be made if a sizable degradation change is noted, verified, and traced to a specific spacecraft event.

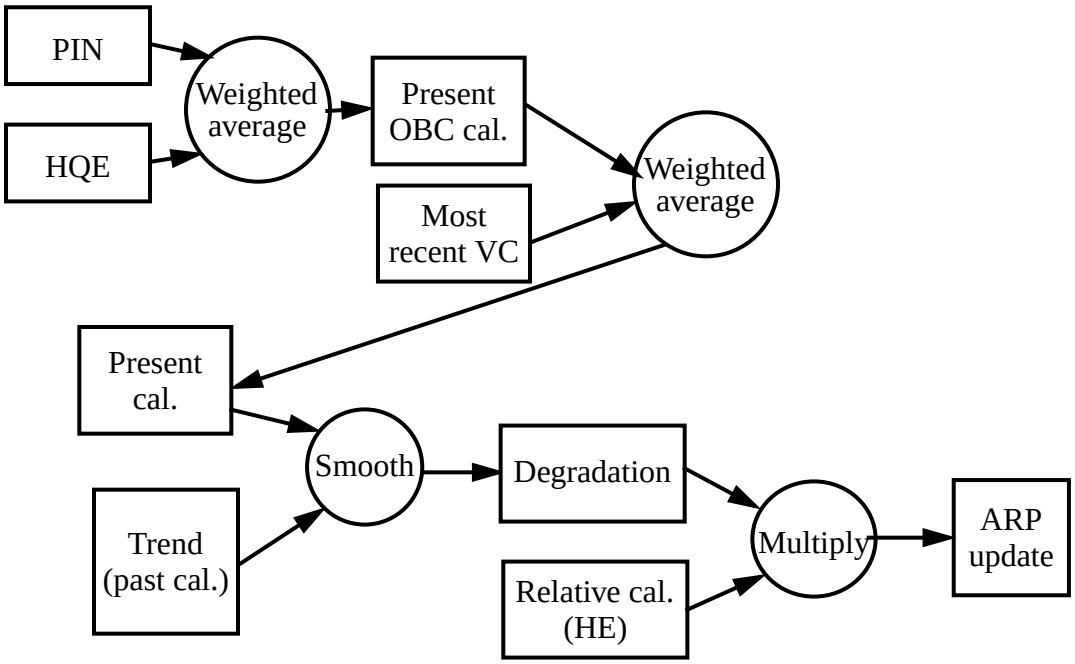

Figure 5.3. Calibration coefficient weighting.

This represents one possible approach to combining the data sets. In the development of a specific algorithm, the Kalman filtering approach[18] will be investigated. This methodology treats the scene, OBC, sensor as a unit, specifying the limits to parameter changes, then adjusting the parameters until a likely systems model is obtained.

As defined in Section 3.3, the response coefficients will be determined from a regression of camera output DN to total band averaged spectral radiance. This is true for each of the calibration methodologies.

5.1 OBC CALIBRATION

During preflight testing, an integrating sphere and the laboratory photodiode standards are utilized to achieve the radiometric calibration of the cameras. In-flight, MISR is calibrated using an On-Board Calibrator (OBC) that consists of two Spectralon diffuse calibration panels, high quantum efficiency (HQE) diodes in a trapped configuration, and single (not trapped) radiation-resistant PIN diodes, including one mounted to a goniometer arm to provide angular characterization of the diffuse panels. Figure 5.4 shows the location of these elements with respect to the optical bench structure.

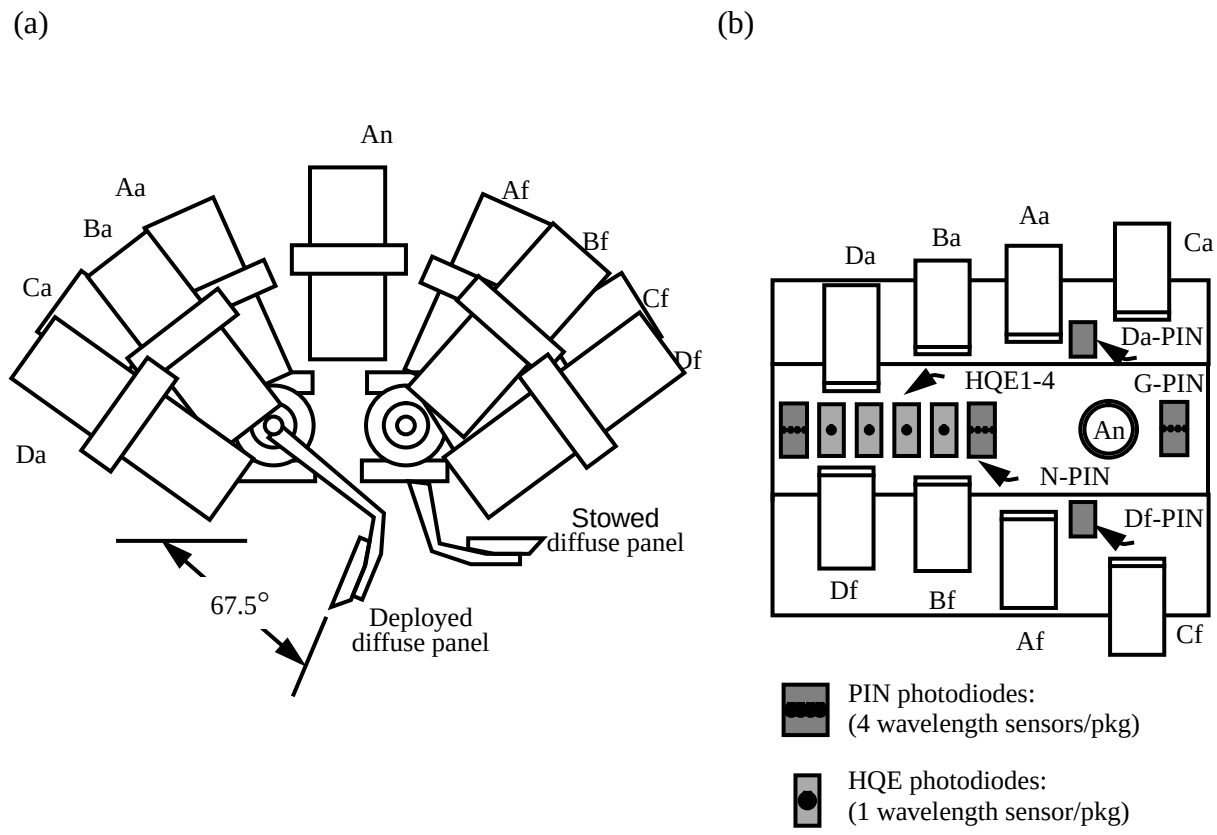

Figure 5.4. Location of a) the calibration panels and b) photodiodes on the optical bench.

The time available for calibration will be about seven minutes at each pole. At the North Pole the cameras will see a range of illumination, through sunrise (sunset at the South Pole) onto the panel, to a view of the Sun through a varying amount of Earth atmosphere (including atmosphere-free space). By using the photodiodes to measure the panel-reflected radiances, the cameras will be calibrated using data covering the dynamic range of the sensor. In addition to these panel views, the cameras will gather data over the dark Earth for three minutes each month, during a new moon. The dark-Earth data will establish the dark current spatial variability across

the array. Dark current is expected to be slowly varying during the mission, gradually increasing due to particle radiation exposure.

Key inputs to the OBC processing algorithm include the panel preflight BRF data base, preflight photodiode calibration data base (relative spectral and absolute radiometric response values, detector area times field-of-view product (AΩ), and external quantum efficiency), as well as the sun angle of illumination for every in-flight photodiode reading.

5.1.1 Diffuse panels

The panels are deployed for calibration at monthly intervals, except at mission start when multiple observations are collected the first month. Over the North Pole, one panel will swing aftward to reflect diffuse sunlight into the fields-of-view of the aftward-looking and nadir cameras. Over the South Pole, the other panel will swing forward for calibration of the forward-looking and nadir cameras. Thus, the nadir camera will provide a link between the two sets of observations. By monitoring the panels with photodiode assemblies, and through consistency checks using overflight campaign data, slow changes in panel reflectance are allowable without compromising the calibration accuracy, since the photodiodes provide the primary standard.

The in-flight calibration panels are required to have a high, near-Lambertian reflectance. These properties are needed to direct sufficient energy into the cameras to reach the upper end of the sensor dynamic range. The Lambertian property also facilitates knowledge of the radiance into the cameras, as the radiance is measured by photodiodes at a particular panel view angle, and corrected for departure from Lambertian behavior. One challenging panel requirement is for uniformity in the reflected radiance field. This is necessary in order to accurately measure pixel-to-pixel, band-to-band, and camera-to-camera differences in responsivity. To fulfill this requirement scattering of light, from the instrument structure, is minimized, and baffles are provided to block the panels from a view of other instrument and spacecraft structures.

After a materials search, Spectralon has been selected as the material of choice for the MISR in-orbit calibration panels. Spectralon is a product of Labsphere (North Sutton, New Hampshire), and is composed of pure polytetrafluoroethylene (PTFE, or Teflon) polymer resin that is compressed into a hard porous white material using temperature and pressure sintering. No binders are used in the procedure. Spectralon is widely used in laboratory and ground/ field operations as a reflectance standard. MISR has provided for the flight qualification of this material[5, 7]. Areas of investigation for flight qualification included static-charge build-up studies, optical characterization, environmental exposure, measurement of mechanical properties such as tension and compression strengths, and vibration testing. The environmental exposure studies were extensive, and included ultraviolet (UV), humidity, atomic oxygen and thermal cycling impact studies. The diffuse panels are stowed and protected while not in use. Cumulative space exposure time (deploy time) for each panel is expected to be less than 100 hours over the mission life. Thus, panel reflectance degradation is expected to be low (changing less than 2% the first year, and 0.5% per year thereafter).

Deployment of the panels, as well as the cover, will be actuated through the use of a mini-dual drive actuator, providing redundancy and fault tolerance. A single motor is used for the

goniometer. Redundancy is not implemented for the goniometer, since its failure would not be mission critical.

5.1.2 Calibration photodiodes

The diffuse calibration panels will be monitored by three types of diodes: radiation-resistant PIN photodiodes and two types of High Quantum Efficiency (HQE) diodes. (Note: "PIN" is a description of the diode architecture where *p*, *i*ntrinsic, and *n* doped layers are stacked.) The radiation-resistant photodiodes will be fabricated four to a package, each diode filtered to a different MISR spectral band. The fields-of-view are approximately 2.7°, sufficient to allow the required signal-to-noise ratio (SNR) of 500 to be achieved. Five such packages will be used. Two will view in the nadir direction, two in the Df and Da camera directions, and one package will be mechanized on a goniometric arm to monitor the angular reflectance properties of the panels.

The HQE's are in a "trap" configuration. Here three silicon photodiodes are arranged in a package so that light reflected from one diode is directed to another diode. The output of each diode is summed, resulting in near 100% quantum efficiency. A single spectral filter per package is used, and four such packages provide coverage at the four MISR wavelengths. One diode type will be used to obtain high quantum efficiency (QE) in the blue, and another type will be optimized for QE in the remaining three bands. The diodes have been specified to have an internal quantum efficiency exceeding 0.995, to have a front surface loss of less than 20%, to have a linearity of response better than 99.99% over an *equivalent reflectance* range of 0.05 to 1.0, and to have SNR in excess of 500 at full scale.

The equivalent reflectance parameter is used to specify instrument signal-to-noise requirements. This parameter is defined as:

$$\rho_{eq} = \pi L_\lambda / E_{0\lambda} \qquad \text{equivalent reflectance}$$

where L_λ is the spectral radiance incident at the sensor while observing a given target, and $E_{0\lambda}$ is the spectral exo-atmospheric solar irradiance at wavelength λ. (Both L_λ and $E_{0\lambda}$ are band weighted over the passband response.) To convert an equivalent reflectance into radiance, therefore, $L_\lambda = E_{0\lambda} * \rho_{eq} / \pi$ where $E_{0\lambda}$ is the exo-atmospheric solar spectral irradiance, as given by the World Climate Research Programme[47].

5.1.3 Goniometer

The goniometer is a mechanized device which characterizes the relative diffuse panel radiance function with angle. It does so in a plane parallel to the spacecraft flight direction. A PIN package mounted to the goniometer arm swings through ±60° to allow panel characterization appropriate to the along-track camera angles.

5.1.4 OBC Uncertainty Analysis

Uncertainties in the OBC calibration methodology come from a range of sources, as itemized in Table 5.1. The budgeted values are the uncertainties anticipated at the onset of the

OBC design effort. The actual uncertainties will be fully documented at the conclusion of the camera preflight test program. The uncertainties will be re-evaluated and updated, as needed, in the post-launch era.

Table 5.1. OBC calibration uncertainty sources

Source	Uncertainty(%) at ρ_{eq}=0.05		Uncertainty(%) at ρ_{eq}=1.0	
	Budget	Actual	Budget	Actual
Diode radiance accuracy	4.8		2.3	
Panel relative BRF	1.0		1.0	
Panel reflectance non-uniformity	1.0		1.0	
Panel glint	1.0		0.5	
Camera SNR	0.1		0.001	
Correction for diode/ camera out-of band differences	1.0		1.0	
Calibration equation approxima-tion to radiative transfer curve	3.0		0.5	
Total Uncertainty (Root Sum of Squares)	6.0		3.0	

5.2 VICARIOUS CALIBRATION

Vicarious calibration (VC) is defined as the use of in situ or non-MISR sensor data to determine the top-of-atmosphere (TOA) radiances at angles viewed by MISR detectors. The relation of the TOA radiances to DNs recorded by MISR provides a point on the calibration curve. As information is not available through the sensor dynamic range, only the first-order response parameter, G_1, can be updated. The advantages of VCs are their duplication of science mode camera geometry during calibration (Earth view, full-aperture illumination at mid-dynamic range, comparable to science data acquisition). Three types of vicarious calibrations will be implemented by the MISR vicarious calibration team. These are discussed below. Error estimates for these will be developed during this program. The sensor cross-comparison, where the radiance measured by a separate satellite sensor as it images the same selected ground scene, is discussed Section 8.1.

All three VC techniques will make use of sunphotometer measurements and a radiative transfer code (RTC). The sunphotometers are solar-tracking radiometers. Measurements are converted to atmospheric transmittances and used to determine the aerosol properties and columnar absorber amounts over the sites[8,9]. Algorithm and sensor validation was conducted during the First ISLSCP Field Experiment (FIFE). (The International Satellite Land Surface

Climatology Project (ISLSCP) is sponsored by the World Meteorological Organization and the International Commission of Scientific Unions).

Sunphotometers available to the MISR vicarious calibration team include Reagan manual and autotracking sunphotometers, as well as CIMEL sunphotometers. These instruments are described in the MISR [Val Plan]. As the Reagan instrument and data reduction techniques have been key to VCs for over a decade, these data will be baseline unless the other measurements are proven to be of greater accuracy. Sunphotometer calibration will include a trending analysis of clear-atmosphere data, taken over the vicarious test sites.

These atmospheric measurements will be used as input to a RTC. The code MISR will used is termed the West RTC, and is based on the adding-doubling method[48]. It will be used to simulate TOA radiances as would be observed by the MISR instrument, for a given choice of aerosol type and amount, and surface reflectance (or upwelling radiance) properties. Eventually the aerosol model to be used for VC computations will be based upon the retrieval work of the MISR aerosol team over our test sites. Other RTC tools, such as use of MODTRAN, will prove invaluable at computing radiance distributions with wavelength. MODTRAN results, if utilized, will be scaled to agree with the monochromatic computations of the West RTC, at wavelengths where the West code is run.

In order to generate TOA radiances, averaged over the MISR spectral band profile, the in-situ measurement approach will be to:

- measure radiances and reflectances in bands simulating the MISR passband;
- characterize the scene spectral distribution of the measured radiances or reflectances; and
- measure atmospheric parameters in narrow bands (~ 10 nm).

Portions of the filter plates constructed for the MISR instrument procurement have been set aside for use in MISR in-situ instruments. These will be used in the field instruments used to measure radiance and reflectance.

The rationale for this is that radiances should be measured using sensors with spectral response profiles matching MISR, where possible (yielding a product simulating the MISR retrieved radiances). When propagating these radiances using a RTC, however, monochromatic radiance, reflectance, and atmospheric parameters are used. To generate RTC input, therefore, a spectral model of the radiances are assumed. The RTC propagates radiance components at discrete wavelength sample points (e.g., every 5 nm throughout the MISR in-band response range, and every 100 nm elsewhere between 365 and 1100 nm). These TOA radiances then need to be interpolated with wavelength, to deliver MISR band-averaged radiances. Radiances representative of all MISR bands and field angles will be computed. The Validation Team will deliver these radiances to the IFRCC team, who will regress them against the corresponding camera DN values to provide the VC coefficients.

5.2.1 High-altitude sensor-based calibration

The VC which utilizes high-altitude sensors is the most accurate. The utilization of a sensor such as AirMISR[13] would be ideal, and is probably the only methodology which will meet our accuracy requirements for all MISR sensor view angles. The method relies on a sunlit, optically stable target being imaged simultaneously by the aircraft sensor and MISR. Cloud-free conditions are required. The airborne sensor views the target at the same geometry as the camera to be calibrated. As several AirMISR passes would be necessary to cover a range of MISR view angles, it is important to understand the deviations in upwelling radiance due to changes in solar illumination angle during the overpass. Small corrections must also be applied to account for the effects of the atmospheric path between the aircraft and the satellite, and to account for the difference between the footprints of the two instruments on the target. Although this technique has the disadvantages of a higher cost and difficulty in scheduling and implementing, it is the preferred vicarious methodology. A semi-annual overpass is planned.

In order to weight radiance-based calibration coefficients against other methodologies, the accuracy of this product must be understood. Additionally, the uncertainty estimates provide input to the MISR radiance retrieval uncertainty estimates. Table 5.2 details the error budget for the calibration of MISR, using the high-altitude radiance-based methodology. The actual uncertainties will be determined prior to VC implementation in the post-launch era.

Table 5.2. High-altitude sensor uncertainty sources (worst case over MISR view angles).

Source	Uncertainty(%) at ρ_{eq}=0.05		Uncertainty(%) at ρ_{eq}=1.0	
	Budget	Actual	Budget	Actual
AirMISR calibration accuracy	5.0		2.5	
AirMISR in-flight sensor stability	0.5		0.5	
Scene Registration	3.0		1.3	
Atmospheric Correction	0.5		0.5	
Observation Geometry	1.0		0.5	
AirMISR/ MISR differences in spectral profile	0.5		0.5	
Total Uncertainty (Root Sum of Squares)	6.0		3.0	

5.2.2 Surface radiance-based calibration

It is proposed that a surface-based radiometer, such as PARABOLA, be used to measure surface upwelling radiance. This technique, while not as accurate as the high-altitude sensor methodology, has cost and implementation advantages. For this reason these data will always be taken, as a backup should there be difficulties in the previous data set. Use of in-situ

measurements in conjunction with the West RTC will propagate the surface measurement to a TOA radiance value. Table 5.3 details the error budget for the vicarious surface sensor radiance-based calibration.

Table 5.3. Surface radiance-based calibration uncertainties, ρ_{eq}=1.0

Source	Uncertainty (%) for D camera		Uncertainty (%) for A camera	
	Budget	Actual	Budget	Actual
Field radiometer calibration accuracy	2.0		2.0	
Field radiometer stability	0.5		0.5	
Differences in radiometer/ MISR spectral profile	1.0		1.0	
Scene spatial sampling (averaging to MISR field-of-view	1.0		1.0	
Scene relative spectral knowledge	1.0		0.5	
Scene relative BRF knowledge	1.0		1.0	
Atmospheric correction	3.0		1.0	
Spectral integration of TOA radiances to MISR band-averaged value	0.5		0.5	
Total Uncertainty (Root Sum of Squares)	4.2		3.0	

5.2.3 Surface reflectance-based calibration

In the previous methodology surface radiances are measured, then propagated to TOA. In the reflectance-based methodology surface reflectance is measured, a model of the exo-atmospheric solar irradiance is assumed, and a double-path (Sun to surface to TOA) radiative propagation computation is made. This latter approach, therefore, does not rely on the accuracy of a calibrated field radiometer, only knowledge of a reflectance standard. Radiative transfer errors are expected to be greater, as a double path computation is needed. The reflectance-based method has a proven history of use since the mid-1980s, being used to radiometrically calibrate the solar-reflective bands of Landsat-4 Thematic Mapper (TM)[10], the Airborne Visible/ Infrared Imaging Spectrometer (AVIRIS)[11-12, 21-40], and other sensors[13,14]. The objective is to characterize the surface and atmosphere at the time of satellite overpass so that the TOA radiances can be inferred. Surface measurements are made for a number of pixels by transporting radiometers across the site and measuring upwelling radiance. Radiances are converted to reflectance through comparisons with measurements of a panel whose reflectance is known. The MISR Validation Team will use Spectralon panels, whose reflectance is known from the PTFE packing density[49]as well as

laboratory measurements. In order to account for surface inhomogeneities over the MISR field-of-view, measurements need to be made over a 3x3 pixel area.

As this technique is the easiest to implement, it will be the first operational VC technique utilized by the MISR team. Although the uncertainty in the reflective-based VC are well documented for the nadir-view case[10], an analysis for MISR's off-nadir view angles will be necessary. Table 5.4 details the error budget for MISR calibration, using the reflectance-based calibration methodology.

Table 5.4. Surface reflectance-based uncertainties, ρ_{eq}=1.0

Source	Uncertainty (%) for the D camera		Uncertainty (%) for the A camera	
	Budget	Actual	Budget	Actual
Reflectance knowledge of field reflectance standard	1.0		1.0	
Field radiometer stability	0.5		0.5	
Differences in radiometer/ MISR spectral profile	1.0		1.0	
Scene spatial sampling (averaging to MISR field-of-view	1.0		1.0	
Scene relative spectral knowledge	1.0		0.5	
Scene relative BRF knowledge	1.0		1.0	
Atmospheric correction	4.0		2.0	
Spectral integration of TOA radiances to MISR band-averaged value	0.5		0.5	
Total Uncertainty (Root Sum of Squares)	4.6		3.0	

5.3 HISTOGRAM EQUALIZATION

The absolute calibration of a pixel can be considered the product of the at-launch array response, array degradation, and relative pixel response. The first two of these is reported at the most responsive pixel of the array, and the third parameter is normalized to this pixel. There are 1504 relative calibration coefficients per band. The relative response refines the measure of the array response to account for local deviations in response, as occur due to filter and detector small scale imperfections, field angle variations, and broad scale transmittance variations of the filter. The latter effect is particularly large for those few filters which were cut along radial lines, as compared to the filter deposition center. Without a relative calibration adjustment, artificial north/ south stripes would appear in the MISR images. Although the OBC can be used to provide both

the absolute and relative coefficients, it provides a more accurate calibration when used to measure degradation of the array as a whole. This is due to the potential for glint sources, as well as back reflections from the camera front optical surface, and other glint sources of light which are unevenly distributed across the panel. For this reason the baseline approach to relative calibration will utilize Earth-scene data in conjunction with histogram equalization techniques. Verification will be done by intercomparing the two approaches.

If several photoactive pixels view the same scene, the radiances determined from their outputs should be equal, regardless of scene brightness. If this is not the case, the calibration coefficients can be adjusted until the radiances agree. This process is complicated in-flight as no two photoactive pixels ever view the same scene. However, we can assume that with a large ensemble of measurements, the distribution of the intensity of the Earth radiation incident on each photoactive pixel will be similar. The distributions will not be identical, but will become more similar the larger the ensemble. This is the basic premise of histogram equalization (HE)[39,40]. In order to eliminate view-angle errors in the technique, the comparison of pixel outputs will be done against a model which varies with field angle.

A HE analysis starts by selecting a sample of full resolution (Local Mode) Earth-scene data covering as much of the range of intensities as possible. The histogram describing the relative frequency of occurrence of each possible count value for each photoactive pixel, can then be compiled. If any pixel within an array is saturated for a given scene observation, that scene is excluded. After the statistics are compiled, the amplitude of each histogram is plotted versus pixel, and fit to equation. The fit determines the expected average histogram amplitude, for a given field angle. Each pixel response parameter is next modified such that they have the same histogram amplitude as predicted from the reference curve.

5.4 TRENDING ANALYSIS

Use will be made of all data sets which provide a calibration within the accuracy requirements established by the MISR [ISR] document. (Thus no calibration will be accepted without an associated error assessment). It is desirable that data products be produced using instrument calibration coefficients which represent the response at the time of data acquisition. It is also desirable that there be no discontinuities in data products that are a result of abrupt changes in these calibration coefficients due to limitations in sampling the response function in time. For this reason MISR will apply a smoothing function to the monthly calibration data sets. After the data are fit to a low-order polynomial curve, the calibration coefficients provided by the data fit are submitted to the DAAC. It is likely that this fit will be re-established each month, using the last dozen (or so) measurement sets. Thus, after each new in-flight calibration activity using the OBC, a new set of coefficients will be computed. These will be submitted to the DAAC prior to the next OBC data acquisition. It is believed that each new coefficient set will vary only slightly from the previous. It is recalled that the instrument is being built to a stability specification of 0.5% limit on response change per month, and 2% change limit per year.

6. LEVEL 1B1 RADIOMETRIC PRODUCT ALGORITHMS

During Level 1B1 processing the incoming DN pixel values are processed to provide band averaged spectral radiances, reported in MKS (meter, kilogram, second) units referred to as SI (Système International). This MISR product generation occurs routinely and continuously at the Distributed Active Archive Center (DAAC). Two processing steps are involved: radiance scaling and radiance conditioning. These are described briefly here, and more fully in the [L1Rad ATB].

6.1 RADIANCE SCALING

This step of the Level 1B1 processing makes use of response parameters of the calibration equation that are determined during sensor radiometric calibration. Processing is done on a per line basis. First, the offset DN, DN_o, is determined for that line from an average of the eight overclock pixels. This value is subtracted from the active pixel value, then the radiance is computed using the equation in Section 3.3. The response coefficients, G_o, G_1, and G_2, are specific to the pixel being processed. In the case of data averaging, where the camera DN values have been averaged before transmission, a specific table of parameters will be used for that averaging mode. It is believed that these tables can be constructed from the unaveraged pixel coefficients. As this will not be verified until system testing this fall, the more general approach is assumed here. (Preflight coefficients are determined from camera data alone, prior to system integration. Thus, averaging mode data are not yet available).

It is recalled from Section 3.3 that the coefficients determined preflight will not need to be adjusted to account for differences in the source color of the sphere. This is due to the fact that the Level 1B1 product reports a radiance averaged over the entire response range of the instrument. An adjustment to a nominal in-band profile is made. Although an out-of-band correction is made for certain Level 2 products, this correction is not provided for in the definition of the response parameters.

The radiances retrieved using this approach are most accurate when the scene approaches that of an ideal target, that is one that is spectrally and spatially homogeneous (as are the calibration targets themselves). For real scene types, radiometric errors are introduced due to pixel-to-pixel nonuniformities (in the case of on-board data averaging), differences in the out-of-band signal, and polarization of the incoming field. These errors will be documented as part of the characterization task.

6.2 RADIANCE CONDITIONING

In radiance conditioning operations, Level 1B1 processing uses the first-order radiances computed above, and makes adjustments on the order of a few percent to account for specific instrument features. PSF deconvolution and in-band scaling are currently the Level 1B1 baseline corrections.

6.2.1 PSF deconvolution

During preflight testing it was determined that the contrast target specification, given in the [ISR], is violated for a 24x24 pixel lake-type scene surrounded by a "land" background. Scattering within the focal plane, primarily between the filter and detector, has been attributed as the cause. The MISR science team has elected to correct for this haloing affect in ground-processing. The algorithm selected is based upon the maximum-likelihood approach. It makes an estimate of the scene, then using the point-spread-function (PSF) for that array, predicts the DN distribution across the array, for that assumed scene. Then, using the ratio of the true measured scene to that of the image predicted from the estimated scene, the estimated scene is updated. It has been shown that this algorithm is computationally efficient, and that the scene is restored within a few iterations. Only a small number of iterations are required because the halo intensities are small, and thus the observed signal is a good first-order approximation to the restored image.

The PSF functions for the line array are obtained by averaging ten PSF measurements across a pixel. Each individual measurement is the result of sub-pixel illumination at various spacious locations across the array. The averaged PSF profile is nearly spatially invariant across the array. A representative, field-independent profile will be used for each array.

6.2.2 Spectral in-band scaling

The differences in spectral in-band response across an array, and from one camera to another, has been measured in the preflight test program. The largest variation occurs for those few cameras where the filter was cut in the radial direction relative to the deposition center during filter fabrication. (Filter uniformity is more uniform along lines of equal radius). Differences in nominal band shape, as compared to the measured per pixel in-band response, can be accounted for by a scale factor applied to the retrieved radiances. This scale factor is the ratio of the solar exo-atmospheric irradiance, averaged over the desired nominal band profile, to the solar exo-atmospheric irradiance averaged by the actual (measured) in-band response profile. The nominal profile will have no response at out-of-band wavelengths. It has yet to be determined if the nominal profile will be constructed as an average, or representative profile from the measured data.

Ideally the out-of-band subtraction would be done prior to the in-band scaling. The processes have been ordered otherwise, to allow the spectral bands to be registered, retrieving scene spectral response information prior to the out-of-band subtraction. Provided the in-band scaling factor is near unity, there is little difference between the desired correction order and that to be implemented. The out-of-band correction is planned as a Level 2 processing step. Thus, this correction can be implemented or not, depending on product need.

6.3 ARP GENERATION

The Ancillary Radiometric Product (ARP) is the primary deliverable from the in-flight radiometric calibration task. It will be maintained throughout the mission, to give an updated account of the instrument radiometric response, as well as other instrument descriptors. Static parameters will be determined from the preflight data alone; other parameters will be updated in-

flight. Generation of the updated parameters will be facilitated by standardized SCF processing algorithms and procedures. Radiance scaling and conditioning will proceed using the updated parameters. Should MISR radiances be reprocessed at some time, the DAAC algorithms will make use of the parameters which best represent the instrument response at the time of data acquisition.

6. Level 1B1 radiometric product algorithms

7. CHARACTERIZATION

The radiance uncertainty estimates reported in the ARP assume an homogeneous target, and will be applicable for the majority of scene types. For some targets, however, the radiance uncertainty may grow. The in-flight characterization program will determine the magnitude of error, under a range of such conditions. The data community can make use of these reports to better assess their scientific products for arbitrary scenes.

The characterization studies conducted by this team are divided into three categories: scene specific errors, noise analyses, and data anomalies. These are discussed respectively in the sections to follow.

7.1 SCENE SPECIFIC RADIOMETRIC ERRORS

The errors described in this section are all predictable from known interactions between the scene and the sensor. That is, with a complete characterization of the scene and sensor, an accurate radiance retrieval can be made. Typically, however, scene information such as relative spectral or spatial distributions are not accurately known without excessive data analyses. For this reason, and because the number of such observations are believed to be small, correction algorithms will not be developed for standard processing. The characterization task gives the uncertainties for these cases in light of our existing implementation approach.

7.1.1 Contrast target

The [ISR] gives specifications for the allowable radiometric error for each of two contrast targets. During the preflight characterization it has been determined that the specification for one of these targets (the 24x24 pixel dark lake with land background) can only be met if PSF deconvolution is included in Level 1B1 processing. As part of the in-flight characterization program, we will further explore the need for the deconvolution approach. A precise deconvolution algorithm and code will be developed. This code may or may not be the same as the Level 1B1 product generation code, in that it will be optimized for accuracy rather than computational efficiency. This code will be used to deconvolve a variety of Level 1A scenes, spanning a range of contrasts and spatial distributions. From this study the difference in radiances between the Level 1B1 product and this best scene estimate will be compiled. With these results the radiometric errors for a range of contrast targets will be reported. In addition, an assessment will be made as to which fraction of the global data set have been improved by the Level 1B1 processing, and which require even further processing.

7.1.2 Spectral errors

The MISR characterization team will evaluate radiometric errors resulting from spectrally inhomogeneous scene types. One spectral error that has been investigated in the past is that due to undetected spectral shifts, as might occur on-orbit. This error could also result from a wavelength knowledge error during spectral response profile determination. For MISR the preflight filter stability results give an estimate of potential spectral shifts, and the preflight spectral response uncertainty analysis gives an estimate of the error in spectral knowledge. The combination of

these is on the order of 0.5 nm. The radiometric error for this slight a shift is quite small, but will be included in any spectral error report.

The more significant analysis to be done is that associated with the development of the in- and out-of-band spectral scaling algorithms. These processing steps do not actually correct for a radiance error, but rather adjust the retrieved radiances to predict what would have been measured with a more ideal spectral response profile. The in-band spectral scaling algorithm corrects for differences in centroid center wavelength and in-band passband shape across the array and from one camera to the next. The out-of-band adjustment subtracts that fraction of the output due to out-of-band response. In the current MISR product generation scheme, the in-band scaling is performed at Level 1B1; out-of-band subtraction is performed upon generation of specific Level 2 products. The out-of-band response correction is postponed until later in the product generation stream so as to allow registration of the four channels in each camera. This permits a crude measure of the scene spectral profile to be estimated and utilized within the retrieval algorithm. The development and validation of both spectral algorithms are the responsibility of the IFRCC team.

This task will evaluate the current correction sequence, as compared to an ideal approach of having band registration (or an AVIRIS-like scene spectral retrieval) available at the time of Level 1B1 processing. Also, the utilization of a representative line profile, rather than a more general data set which characterizes the field angle differences, will need to be evaluated.

Three data sets are identified for this work. First, a set of registered Level 1A data are needed. This product is not available as a DAAC product, and will need to be generated at the SCF using code developed for us by the Science Data System Team. Second, AVIRIS data are to be used in this study, as they provide samples of complete scene spectral distributions. MISR will work with the JPL AVIRIS team for a data exchange which will provide these data sets. Finally, a typical MISR global data set will useful in evaluating the fraction of global data subject to these reported worst-case spectral errors.

7.1.3 Pixel non-uniformity

On-board averaging results in a radiometric error for scenes of high spatial contrast across the pixels being averaged. Preflight testing has determined that the mean pixel response difference, piecewise across four-pixel blocks, is less than 1%. With this uniformity, it is rare that significant errors will be incurred due to on-board averaging. There are, however, a half-dozen or so pixels per line which have response variations exceeding the 3% specification. Corrections for these non-uniformities could be made, by using the high-resolution An (nadir) camera to measure the relative surface inhomogeneity. This scene information could be used to correct errors introduced during data averaging. Although it is not possible to implement this approach in Level 1B1 processing, a registered data set can be provided as a special request to the SCF. Thus, a comparison of the actual versus desired approach can be evaluated. The evaluation of a second approach, where the high-resolution red band data are used to infer scene inhomogeneity at other wavelengths, has also been proposed. Unless there is a need to incorporate pixel non-uniformity correction within the standard processing algorithm, the more exacting approach will be used to evaluate the radiometric errors due to this instrument-induced effect.

7.1.4 Polarization

MISR has been designed to be insensitive to the incoming state of polarization to within ±1% (1σ). Preflight testing has confirmed that the design has been implemented correctly, and that this specification has indeed been met. A summary of this study will be referenced in any in-flight characterization report which attempts to document all scene-type errors. Verification of camera polarization insensitivity will not be repeated post-launch.

7.2 NOISE STUDIES

The IFRCC team will develop algorithms to document noise within the imagery, and to classify the noise as coherent or random noise. Further, the signal-to-noise ratio (SNR) over a range of radiances will be measured throughout the mission. A combination of dark and illuminated scenes will be processed using these algorithms, and summary reports will provide these results to the user community. These studies are summarized in Figure 7.1.

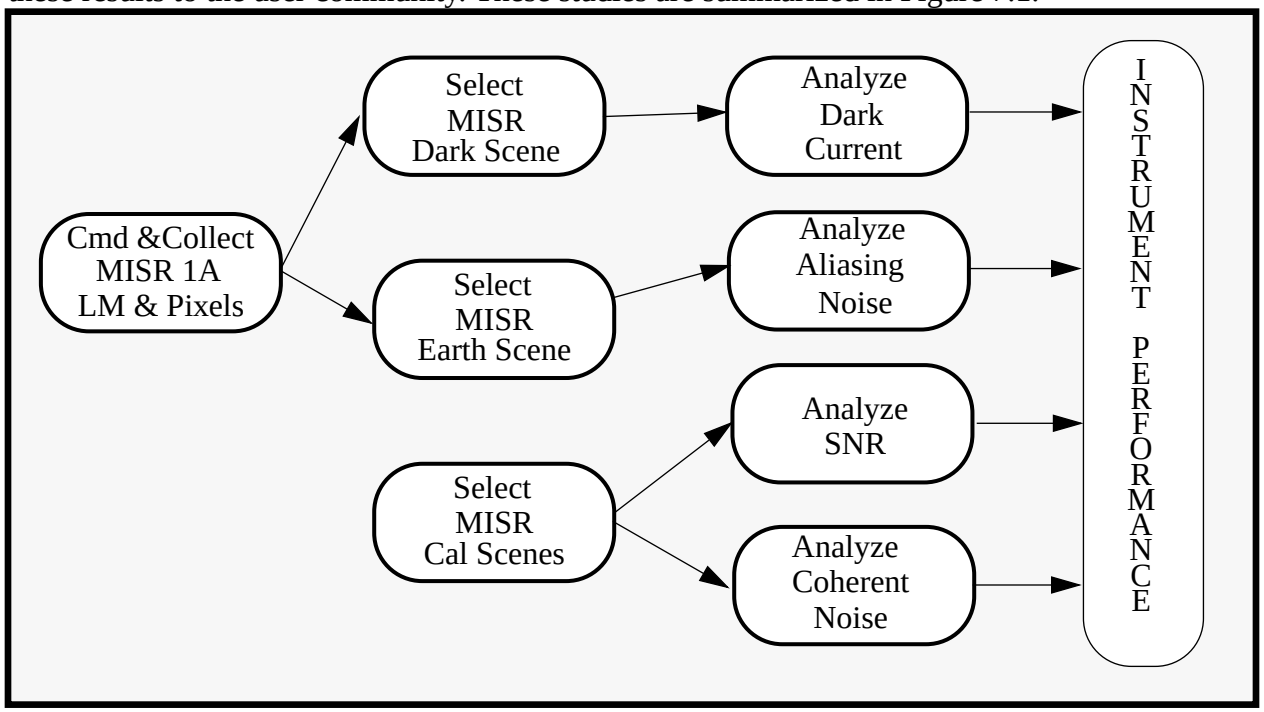

Figure 7.1. Noise Analysis

7.2.1 Dark current

Dark current has been measured at about ±1 DN, during preflight camera testing. At this level it is an insignificant source of noise. This will additionally be verified during instrument and observatory (spacecraft) environmental testing. It will also be monitored on-orbit as part of the monthly calibration sequence. For this experiment, high resolution data will be collected for 1.5 minutes, on each of the forward and aftward banks of cameras, over the dark Earth. Means and standard deviations, and comparisons to the overclock average will flag any change in instrument performance.

7.2.2 Coherent noise

Coherent noise is characterized by a diagonal striping pattern which appears particularly noticeable in areas of nearly uniform radiance. The Fast Fourier Transform (FFT) has been used to detect and quantify coherent noise effects in the image data from Landsat's Multispectral Scanner System (MSS) and TM[41,42]. These same image techniques will be used in both the system-integration and on-orbit characterization of the instrument.

7.2.3 Aliasing noise

Aliasing occurs because natural scenes are not frequency band limited, and because MISR's frequency response extends beyond the sampling bandpass. The sampling process causes high spatial frequencies beyond the sampling bandpass to fold into lower spatial frequencies within the sampling bandpass. When the aliased, sampled image is produced, there is the potential for significant image degradation. Aliasing can be treated as a signal-dependent, additive noise, and is calculated from the Fourier transforms of the scene and the PSF[43-45]. Fidelity metrics can also be computed to monitor the nature and extent of aliasing associated with a system. Such metrics include an aliased Wiener energy spectrum that represents the sum of all the out-of-band scene energy which has been passed by the image formation process and then folded back into the sampled bandpass. These tools will be developed and utilized by the IFRCC team to report on the nature and extent of aliasing noise within the Level 1B1 MISR data products.

7.2.4 Signal-to-Noise Ratio

Preflight testing has verified that SNR requirements have been met for the MISR cameras. In fact, the cameras appear to be exceedingly quiet and are photon limited with respect to noise. In order to characterize SNR for the flight environment, diffuse panel observations during the monthly calibration sequences will be used. Data from each of the 1504 pixels, and from each of the 36 channels, will be independently evaluated. SNR will be computed from the mean signal (over a time window of 100 data lines) divided by the standard deviation of this same signal. Corrections for solar angle illumination changes will be made, as needed. The SNR computation will be repeated over several time blocks, covering a range of radiance levels.

7.2.5 Offset uncertainty

The offset DN for each line array varies dynamically with average array illumination. At high values (near, or beyond saturation) there additionally appears to be a spatially varying component to the offset. This is evident by inspection of the 536 overclock pixels which are read during camera testing. Under near saturation conditions the signal ramp observed in the overclock is as large as 25 DN, for the near-IR band. It is less for all other bands. There is no way to specifically measure the variability of this baseline across the active array, but it is believed to be no more than the 25 DN observed in the overclock. This is borne out by the fact that the sensors appear to be linear at the upper end of the dynamic range. It will not be possible to further study this error source once the sensor is integrated into an instrument, as only a subset of the overclock pixels are clocked out by the instrument electronics.

It is believed that the evaluation of offset uncertainty will best be made by analysis of preflight test data. These studies will continue over the next year, and be referenced by any in-flight characterization report which review all scene specific errors.

7.3 DATA ANOMALIES

Data anomaly studies are those investigations reporting on cases where information was lost, or data quality degraded by some mechanism not predicted from the physics of the optical train and detector package. These are typically due to features within the electrical portion of the signal train, following detector photon to electron conversion.

7.3.1 Bright target recovery

During preflight testing it was determined that a specific bright to dark target observation could lead to a loss of data for several line times. This effect is greatest when the near-IR band is illuminated with a large input across the array. This causes the offset DN to grow. If now the scene abruptly transitions to a dark target, the offset DN does not instantaneously adjust, and may be larger than the light-proportional component of the signal. A zero output is observed for three line times, resulting in a loss of data for this time interval. It takes the offset about 25 line times to stabilize to its new steady-state value. During this non-zero interval there is no data loss.

The IFRCC team will investigate the impact of this camera feature on the MISR data product.

7.3.2 Saturation recovery

Preflight testing has confirmed that the sensor recovers within a line time, in going from a saturated, to unsaturated scene. Post-launch data analysis will confirm this.

For a partially saturated array, there will be a degradation in the data quality for tens of pixels past the saturated pixel. Data elsewhere in the line are of good quality. The IFRCC team will confirm this feature in the on-orbit data, and develop the proper data quality flag.

7.3.3 Channel-stop illumination

As discussed in Section 4.2.7, under specific illumination conditions a pixel can have a data loss. This occurs when the channel-stop of the preceeding pixel is illuminated. This phenomena will be identified in the data. The IFRCC team will assess the frequency of this occurrence in the data.

7.4 MTF/ CTE STABILITY

High contrast scene data will be utilized to validate the stability of CCD charge transfer efficiency (CTE) and MTF throughout the mission. For CTE studies, statistics will be compiled to evaluate the contrast observed using pixels at one end of the array, as compared to the other.

7.5 LOCAL MODE TARGET SELECTION

In order to conduct the above investigations, MISR will routinely make use of Level 1A Science data, particularly those images acquired in Local Mode (LM). These targets can be categorized into the following groups:

- high contrast scenes, including lakes and cloud over ocean scenes; and
- intensive vicarious field campaign sites;
- stable desert regions;
- spectrally interesting scenes (e.g. vegetation)

The IFRCC Team will work with the Science Team in the selection of LM sites.

8. CALIBRATION INTEGRITY

Calibration integrity is the IFRCC program element that validates the Level 1B1 Radiometric Product, as well as the out-of-band correction which occurs at Level 2. It also provides for quality assessment, and demonstrates traceability of the radiance scale to international standards. These tasks are described in this chapter.

8.1 LEVEL 1B1 RADIOMETRIC PRODUCT VALIDATION

Validation confirms that Level 1B1 DAAC processing is generating radiances per the formulism of the [L1Rad ATB] and per the accuracy requirements specified in the [ISR]. The process of generating radiances using multiple methodologies is in itself a validation. The radiances derived from the OBC and VC approaches are completely independent, and thereby establish both the response of the sensor, and uncertainties in using these response coefficients to measure incoming radiances.

There are several validation approaches to be developed by the IFRCC team: that of a sensor cross-comparison, desert scene views, and lunar observations. Whereas the approaches described in Chapter 5 provide a continual check on the reported product, these latter analyses are not routine. Development for these latter tasks will begin once the in-flight calibration and characterizations tools are fully developed. That is, these are activities which will be developed post-launch. At most one sensor cross-comparison (per sensor) will be made each year. Desert scene data will be collected and summarized, as available from cloud-free, Local Mode observations. Lunar observations are mentioned here only for completeness. The analysis of these data actually have not been planned for at this time, due to the uncertainty of their availability.

8.1.1 Sensor cross-comparison

In-flight cross-calibration between sensors can be conducted when the sensors have:

- Similar spectral bands that cover part or all of the same spectral range and image the same scene simultaneously but with different IFOVs; for example ASTER, MISR, and MODIS.

- Similar spectral bands and IFOVs but do not image the same scene simultaneously; for example, MISR, Landsat-TM, and SPOT.

No attempt will be made to calibrate MISR by these techniques, as other sensors are not calibrated to the 3% accuracy of MISR. Further, the transfer of calibration from one sensor to another is less accurate than calibrating a sensor directly. What can be determined, however, is the radiance bias to within a 7-10% range of uncertainty. This will be done, particularly between MODIS and MISR sensors. MODIS is the preferred sensor to establish a cross-comparison with, as

- MODIS is on the same platform, and a cross-comparison will add value to the products making use of the synergy of data sets;

- MODIS has bands similar to the four MISR bands, which will facilitate the cross-comparison;

- a measure of the bias between radiance scales will be made preflight. This latter work is facilitated by the round-robin experiments where a transfer radiometer compares the MISR and MODIS laboratory standards.

Difficulties in comparing MODIS and MISR radiances occur primarily due to band shape differences, and the nature of the radiance product[17]. MISR will report in-band weighted radiances, whereas MODIS will report the total detected radiance. This necessitates the selection of reference sites that are as spectrally neutral as possible, in addition to being of high spatial uniformity over 3x3 pixel areas. Prior to the comparison, MISR will condition MODIS radiances to estimate the radiances MISR would report, per our formulism.

Although of lower accuracy, the cross-calibration of sensors on different platforms is of importance in at least two cases: 1) to cross-calibrate two models of the same sensor (e.g. MISR-AM1 to MISR-AM2), 2) to cross-calibrate sensors that are providing long-term global-change data sets. MISR will support these studies, as the need arises.

8.1.2 Desert scenes

Stable desertic sites have been used for the calibration verification of optical satellite sensors. By assuming a surface and atmospheric climatology, radiances can be computed without the overhead of intensive field campaigns. The SPOT team has investigated 20 desertic zones selected in Saharan North Africa and Saudi Arabia[46], selected using a criterion of spatial uniformity in a multitemporal series of cloud-free METEOSAT-4 visible images. For these scenes they have verified the temporal stability of these sites at hourly and seasonal time scales. We plan to make use of these desert sites in the verification of MISR radiometric calibration.

8.1.3 Lunar observation

The Moon cannot be viewed by the MISR sensors unless there is dedicated lunar/ deep space Calibration Attitude Maneuver (CAM). The MISR instrument was designed to meet its performance specifications without the reliance on any CAMs. Since the Moon is not an extended target sufficient to fill the MISR field-of-view, and because lunar observations are potentially in different instrument configurations than during Earth observations (i.e., instrument temperatures may be different because the instrument radiators usually face the Earth), we do not consider that lunar views will provide any enhancement to the absolute radiometric calibration of MISR. In addition, the Moon provides a single radiance level at the lower end of the MISR dynamic range; a full calibration of MISR requires measurement at multiple radiance levels. On the other hand, a lunar CAM can provide an independent stability verification, thus enhancing our confidence that the strategy we have adopted is working, and the values we quote for radiometric uncertainty are valid.

The baseline CAM is the most useful maneuver to MISR, relative to other lunar CAM's that have been discussed, for two principal reasons. First, the continual pitch motion provides a view of the Moon in all nine of MISR's cameras, as well as the calibration diodes. A pitch hold maneuver, for example, would provide a lunar view in only the nadir camera. Secondly, the MISR camera line arrays resolve the lunar disk, and pitch hold provides only a single line of imagery in each of the nadir camera bands; the location of this line is uncertain by 2.5 arcmin out of the 31 arcmin lunar diameter due to uncertainties in the spacecraft attitude control system. Thus, there would be no way to guarantee that repeated looks at the Moon were seeing the same spot on the lunar disk. On the other hand, continual pitch motion, as provided by the baseline maneuver, provides pushbroom imaging of the entire lunar disk, and repeated looks at the Moon can therefore be co-registered using the lunar limb and features on the lunar disk. This is essential if we are to use the Moon as a stability monitor.

Observations of the sharp edge of the lunar limb also provide benefit in verifying the stability of the instrument point spread function and modulation transfer function response. Accumulated charged particle radiation damage to the CCD's in the MISR cameras are expected to degrade their charge transfer efficiency over the lifetime of the mission, for signal levels below 10% equivalent reflectance. Since most dark scenes observed by MISR (e.g., the open ocean) are spatially uniform, this degradation should not adversely impact the experiment science objectives. However, periodic observations of the Moon will enable a characterization of this effect relative to an early mission baseline, and provide greater confidence in our understanding of how stable the instrument performance is with time.

8.2 QUALITY ASSESSMENT

The MISR approach to quality assessment (QA) has elements performed by the DAAC Product Generation System software, and also by the IFRCC team at the SCF. It will be an automated process, with human involvement limited to spot checking of the data stream, and anomaly investigations[15].

The first quality indicators are reported as metadata files during Level 1A processing. Separate quality indicators are reported for conditions where:

- A pixel falls below the offset DN (as measured by the overclock average);
- A pixel is saturated;
- A pixel is within an array where a saturated pixel was clocked out previously.

For the first two of these there is a data loss. For the third case there is an uncertainty in the data, which decreases with increasing scene signal. That is, the relative radiometric error caused by the spatial blooming of a neighboring saturated pixel, depends on the signal observed by that pixel. If the signal is high, then the addition of a potentially large (e.g., 100 DN) noise is less consequential.

The QA indicators for Level 1A are reported as Level 1A metadata. These indicators are available to all downstream processes.

At the SCF an in-depth analysis of the analysis and software results will be done for samples of data taken from the Level 1B1 product. Statistical summaries of the radiometric QA flags, reported in the Level 1A metadata files, will be prepared by the IFRCC team.

8.3 TRACEABILITY

For both the preflight and in-flight calibrations, MISR output are radiometrically calibrated using a spatially uniform source whose radiant output is determined using detector standards[6]. Source standards rely on a series of radiometric comparisons, as provided by the National Institute of Standards and Technology (NIST) or other standards laboratory, through a lamp vendor, and to the instrument flat-field calibration source. Conversely, detector standards are based upon knowledge of photon to electron conversion efficiency, filter transmittance, and acceptance cone of illumination. It is believed that the MISR detector standards provide greater radiometric accuracy than would be obtained using source standards.

Verification of the MISR radiance scale is provided through

- using NIST traceable filter standards to verify calibration of the photodiode filter transmittance;
- sending the MISR laboratory standards to NIST for radiance calibration and field-of-view mapping (done following MISR shipment); and
- supporting round-robin verifications of our preflight sphere source.

An example of the latter verification was the round-robin cross-comparison experiment of August 1994. At that time several members of the Earth Observing System (EOS) calibration panel brought their detector standards to Jet Propulsion Laboratory (JPL). These were used to sequentially view the JPL integrating sphere. Participating were calibration scientists from the Optical Sciences Center, University of Arizona; National Research Laboratory of Metrology (NRLM), the Japanese standards laboratory; and Goddard Space Flight Center (GSFC).

In order to intercompare observations from these three detectors, a means of extrapolating measurements at one particular instrument's bandpass, to that observed by another instrument with a different band profile was needed. It was decided to use the JPL observations to calibrate a sphere output model[1], and in turn compare the visitor observations to this model. The utility of the model was simply to provide the wavelength interpolator needed to intercompare the various spectral observations. Next, the visitor radiance observations were compared to this model. A summary of the detector intercomparison observations is given in Table 8.1. The number of wavelength intercomparisons was limited because only the Band 2 MISR detector standard was available at this date, and the NRLM radiometer is a single channel. The particular level studied

had all lamps on, and the satellite sphere aperture fully open. With agreements being better than 1%, we have gained confidence in our fundamental approach.

Table 8.1. Radiances [W m^{-2} sr^{-1} μm^{-1}] as compared to the sphere model, and percentage deviation.

Wavelength (nm)			
Radiometer	550	650	666
MISR	612. (0.4%)		
UofA	584. (1.%)		934 (-0.8%).
NRLM		(909) 0.9%	

8. Calibration integrity

9. MANAGEMENT

9.1 PERSONNEL ROLES

9.1.1 IFRCC team

The IFRCC team are those individuals who will assume primary responsibility for tasks described in this plan. These individuals are:

- Instrument Scientist. The Instrument Scientist will manage the IFRCC team. To that end she will develop a detail schedule of activities, track milestones, and determine the best allocation of resources in order to accomplish the identified objectives. She will be responsible for the documentation and reporting of team activities to the EOS community, and will represent the group at EOS calibration workshops. She will also represent the principal investigator, as needed, in matters concerning the instrument science performance.

- Algorithm Developers. Algorithm developers will provide investigations and simulations as needed to develop IFRCC algorithms. They are additionally responsible for the analysis of instrument data, as needed to characterize and calibrate the camera through preflight testing and integration. Responsibilities will include:

  - the development of an algorithm to utilize the panel BRF data base and provide the translation of photodiode-measured radiances into camera incident radiances;

  - the development of the radiometric calibration methodology weighting scheme;

  - the development of the PSF deconvolution algorithm;

  -the development of the spectral response correction algorithm; and

  - a determination of the consistency of camera and photodiode response to a given scene, using data acquired during system testing.

- Software Subsystem Development Engineer. The software subsystem development engineer is responsible for establishing software requirements, designs, test plans, and test procedures. He is responsible for implementation, integration, documentation, and delivery of the software subsystem.

- Software Developer. The software developer is responsible for providing the needed code for the in-flight calibration and characterization data analysis. He will also be responsible for the data management and archive.

9.1.2 Resources external to the IFRCC team

Other MISR individuals key to the IFRCC task are listed below. The personnel and team relationships are summarized in Figure 9.1.

- Principal Investigator. The Principal Investigator has the primary responsibility for all aspects of the MISR experiment, including science algorithm development, data management, calibration, validation, and data archiving.

- Data System Manager. The Data System manager is responsible for the SCF data facility, and additionally serves as the interface for DAAC operations.

- Validation Scientist. The Validation Scientist is responsible for the analysis, error estimates, and reporting of MISR radiances, needed as input to vicarious calibration.

9.2 WORK PLAN

9.2.3 Task and schedule

The task and schedule information is provided in the attached chart (Table 9.1). This schedule is to be further developed and updated through out the program to reflect progress and identify needs. Tasks are further described within this chapter.

Table 9.1 IFRCC task listing

Phase A (present - 1/97)	Phase B (1/97-10/97)	Phase C (10/97-postlaunch)
Planning and outreach		
IFRCC Plan		
Science Data Validation Plan		
EOS Validation Review		
L1Rad ATB		
IGARSS'96 (publish IFRCC plans)		
Functional Req. Doc.		
Software Requirements Doc.		
IFRCC ATB		
SPIE Denver (preflight spectral cal.)		
Software Design Doc.		

Table 9.1 IFRCC task listing

Phase A (present - 1/97)	Phase B (1/97-10/97)	Phase C (10/97-postlaunch)
EurOpto (preflight radiometric cal.)		
I&T activities		
Diodes calibrated		
Camera performance review		
Preflight data archive		
EOS sphere round robin exp.		
System test		
Preship review		
	Ship	
		Launch
OBC cal. software dev.		
Panel BRF data base		
OBC cal. prototype (using system test data)		
Vicarious cal. software dev.		
RTC dev. for reflectance input		
Sunphotometer algorithm		
Railroad Valley exp.		
Radiance bandpass integration		
	VC methodology uncert.	
	VC cal prototype	
	RTC dev. for radiance input	
	RTC input. for high-altitude input	
L1Rad algorithm dev.		

Table 9.1 IFRCC task listing

Phase A (present - 1/97)	Phase B (1/97-10/97)	Phase C (10/97-postlaunch)
PSF deconvolution algor.		
Spectral correction algor.		
IFRCC algorithm dev.		
	Histogram equalization	
	Cal. methodology weighting	
	Noise analyses	
Calibration integrity		
Quality indicators finalized		
		MODIS cross-comparison
		SPOT cross-comparison
		Desert scenes

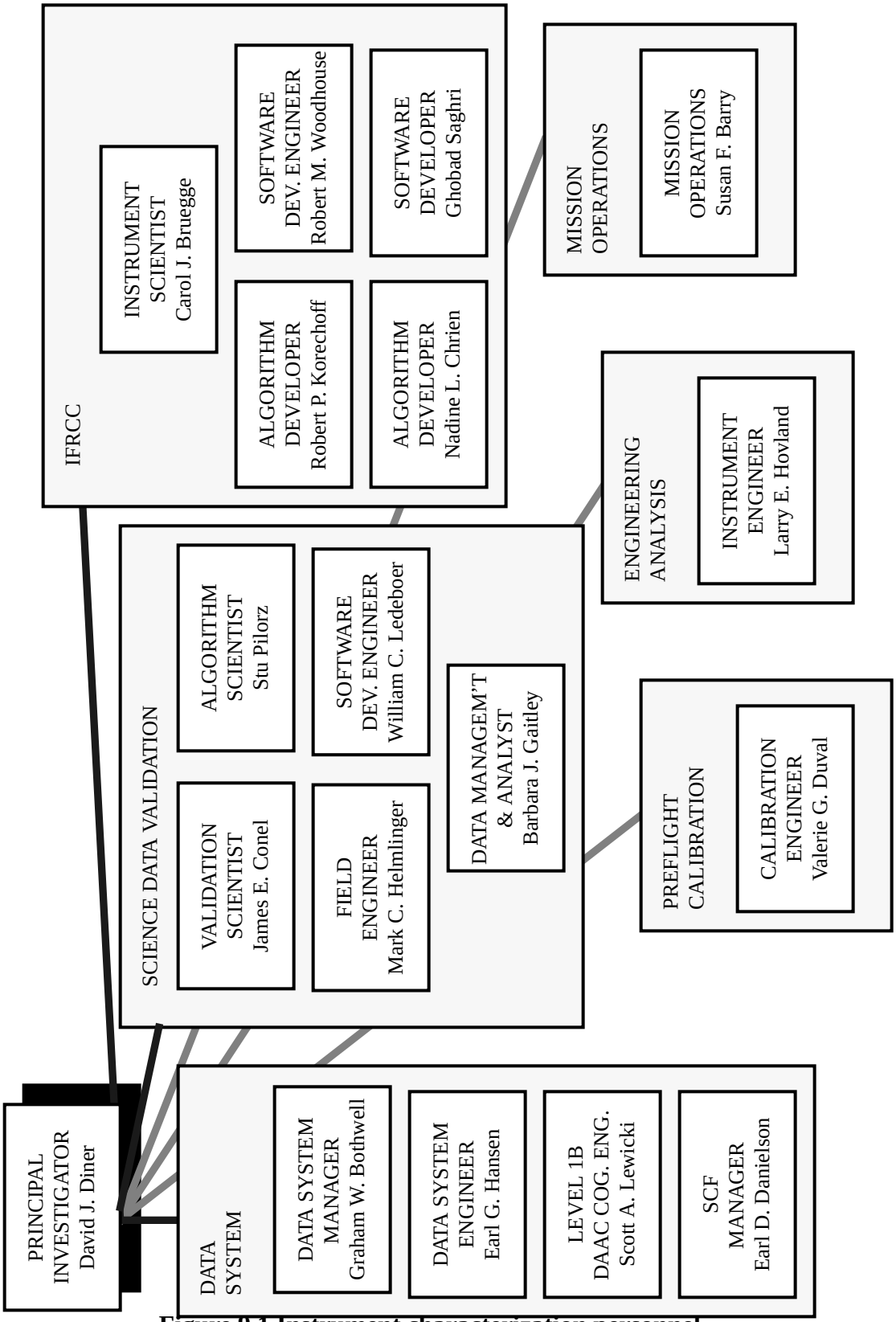

Figure 9.1 Instrument characterization personnel.

9.3 SOFTWARE DEVELOPMENT APPROACH

The software and procedures for reducing MISR instrument data, to provide the in-flight calibration and characterization, are being developed as a unified system, running at the MISR SCF. The overall objective of this effort is to create a data analysis system that will:

- Ensure, through appropriate data management, that the needed data sets are cataloged and accessible to the algorithm developers and data analysts;
- Automate the data analysis algorithms where possible, and provide user-friendly, efficient tools needed in the production processing of large data volumes;
- Provide documentation detailing the data analysis algorithms, code descriptions, and code procedures;
- Maintain the required traceability and modification history between software versions; and
- Produce visual aids and numeric descriptors of instrument performance as needed for the calibration and characterization reports.

The software will be developed using a phased delivery and using software interface tools (e.g.: IDL) as well as standard software languages (e.g.: C, FORTRAN). This software development will follow standard practices (e.g.: JPL D-4000). The software implementation will be preceded by a rapid prototyping phase to take advantage of data generated during system testing. Insight into the subsystem interfaces, graphical user interfaces, and data processing algorithms resulting from the prototyping effort will be incorporated into the final calibration software design. Software documents will outline planning, requirements, software specifications, software design, and software test.

Development phases will include requirements analysis, system design, prototyping/ implementation, testing, documentation and maintenance.

9.3.4 Requirements analysis

The requirements analysis will encompass the entire IFRCC program timeline, to ensure that potential conflicts between short-term and long-term needs are avoided. The initial activity will focus on:

- Ensuring that the software system definition is complete and correct;
- Defining the boundary for the data analysis process, including all external interfaces (e.g. defining the roles and partition of work between the IFRCC team and others, such as the ground support terminal software engineer, flight software engineer, and test conductors in the preflight era, as well as the mission operations team post-launch);

- Identifying/specifying all of the IFRCC outputs that must be produced;
- Identifying which tasks will be accomplished by batch or interactive software and which require procedures;
- Determine the appropriateness of unique software development versus commercial-off-the-shelf-software;
- Producing a Functional Requirements Document; and
- Producing a Software Requirements Document.

9.3.5 System design

The Software Development Engineer will design the software system following completion of the requirements analysis phase. The goals of the system design will be:

- To create a modular system that can be easily adapted to changes in algorithms or required products; and
- Producing a Software Design Document.

9.3.6 Prototyping / Implementation

The Phase A development (through 1/97), will deliver a full prototype system with the following capabilities:

- Finalize the archive of preflight camera, and OBC component (photodiode and diffuse panel) data bases, including electronic archive of design files memorandums reporting camera performance, and analysis procedures;
- Establish the relationship between panel BRF, photodiode output, and camera incident radiances;
- Ingest and archive OBC data sets from system testing, simulating an OBC calibration;
- Finalize the selection of Local Mode scene types required for instrument characterization studies;
- Ingest and archive a vicarious radiance data set, simulating a VC calibration; and
- Finalize algorithm development for radiance scaling, PSF deconvolution, and spectral correction and all other DAAC processes.

The Phase B development (through 10/97) will finalize procedures and software to establish the in-flight instrument calibration and radiance retrievals, including:

- Develop the relative calibration algorithms, including histogram equalization;

- Develop a calibration methodology weighting scheme, evaluating the Kalman filter approach, and trend analysis;

- Develop the needed tools for instrument noise assessment and other characterizations.

Phase C (to post-launch) will focus on the Calibration Integrity tasks, including cross-comparison and desert calibration algorithms.

9.3.7 Test

Testing of the data analysis system will, at a minimum, include:

- Verification of new and previously developed data reduction codes through appropriate intercomparison of results using equivalent inputs; and

- Verification of the integrated system by comparison with separate, independent execution of the individual modules.

9.3.8 Documentation and delivery

Documentation of the validation software will include:

- Functional Requirements Document.

- Software Requirements Document.

- Software Design Document

- User's Guide

The first production version of the system will be delivered to the SCF prior to launch.

9.3.9 Maintenance and revision

Maintenance and revision of the software will be the responsibility of the IFRCC subteam.

9.3.10 Archiving of results

The IFRCC team will deliver routine and special process reports to the MISR Science Design File Memorandum archive. General instrument performance reports will be prepared covering the calibration and calibration trend, radiance retrieval uncertainties, noise, and quality indicators. These will be accessible through the MISR Home Page, as well as open literature publications.

10. REFERENCES

10.1 MISR EXPERIMENT

(The papers in this section have been written by first authors who are currently MISR team members, or who were funded by MISR to conduct the reported study.)

10.1.1 Preflight analysis

1. Bruegge, C.J., V.G. Duval, N.L. Chrien, and R. P. Korechoff. MISR instrument development and test status. In *Advanced and Next-Generation Satellites*, EUROPTO/ SPIE Vol. **2538**, pp. 92-103, 25-28 September 1995.

2. Korechoff, R.P, D.J. Diner, D.J. Preston, C.J. Bruegge. Spectroradiometer focal-plane design considerations: lessons learned from MISR camera testing. In *Advanced and Next-Generation Satellites*, EUROPTO/ SPIE Vol. **2538**, pp. 104-116, 25-28 September 1995.

10.1.2 MISR calibration approach

3. Bruegge, C.J., D.J. Diner, and V.G. Duval. The MISR calibration program. J. Atmos. and Oceanic Tech., EOS special issue, Vol. **13** (2), 286-299, 1996.

4. Chrien, N.C.L., C.J. Bruegge, and B.R. Barkstrom. Estimation of calibration uncertainties for the Multi-angle Imaging SpectroRadiometer (MISR) via fidelity intervals. In *Sensor Systems for the Early Earth Observing System Platforms*, Proc. SPIE **1939**, 114-125, April 1993.

10.1.3 On-Board Calibrator design

5. Bruegge, C.J., A.E. Stiegman, R.A. Rainen, A.W. Springsteen. Use of Spectralon as a diffuse reflectance standard for in-flight calibration of earth-orbiting sensors. Opt. Eng. **32**(4), 805-814, 1993.

6. Jorquera, C.R., V.G. Ford, V.G. Duval, and C.J. Bruegge. State of the art radiometer standards for NASA's Earth Observing System. Aerospace Applications Conference, Snowmass, CO., 5-10 February 1995.

7. Stiegman, A.E., C.J. Bruegge, A.W. Springsteen. Ultraviolet stability and contamination analysis of Spectralon diffuse reflectance material. Opt. Eng. **32**(4), 799-804, 1993.

10.1.4 Vicarious calibration

8. Bruegge, C.J., J.E. Conel, R.O. Green, J.S. Margolis, R.G. Holm, and G. Toon. Water-Vapor Column Abundance Retrievals During FIFE. J. Geophys. Res., Vol. **97** (D17), 18759-18768, 1992.

9. Bruegge, C.J., R.N. Halthore, B. Markham, M. Spanner, and R. Wrigley. Aerosol Optical Depth Retrievals Over the Konza Prairie. J. Geophys. Res., Vol. **97** (D17), 18743-18758, 1992.

10. Bruegge (Kastner), C.J. In-flight absolute radiometric calibration of the Landsat Thematic Mapper. Ph.D. dissertation, Univ. of Arizona, 1985.

11. Conel, J.E., R.O. Green, R.E. Alley, C.J. Bruegge, V. Carrere, J.S. Margolis, G. Vane, T.G. Chrien, P.N. Slater, S.F. Biggar, P.M. Teillet, R.D. Jackson and M.S. Moran. In-flight radiometric calibration of the Airborne Visible/Infrared Imaging Spectrometer (AVIRIS). In *Conference on Recent Advances in Sensors, Radiometry, and Data Processing for Remote Sensing*, SPIE Orlando, Florida, **924**,4-8 April 1998.

12. Conel, J.E., G. Vane, R.O. Green, R.E. Alley, V. Carrere, A. Gabell and C.J. Bruegge. Airborne Visible/Infrared Imaging Spectrometer (AVIRIS): In-flight radiometric calibration and the determination of surface reflectance. Proc. 4th Int'l Coll. on *Spectral Signatures of Objects in Remote Sensing*, Aussois, France, ESA SP-287, 293-296, 18-22 January 1988.

13. Conel, J.E., R.O. Green, G. Vane, C.J. Bruegge, R.E. Alley, and B.J. Curtiss. Airborne Imaging Spectrometer-2: Radiometric and spectral characteristics and comparison of ways to compensate for the atmosphere. SPIE 1987.

14. Conel, J.E., R.O. Green, G. Vane, C.J. Bruegge, R.E. Alley, and B.J. Curtiss. AIS-2 radiometry and a comparison of methods for the recovery of ground reflectance. In *Proceedings of the Third Airborne Imaging Spectrometer Data Analysis Workshop*, JPL Publication 87-30, pp. 18-47, 1987.

10.1.5 Quality assessment

15. Kahn, R., K. Crean, D. Diner, E. Hansen, J. Martonchik, S. McMuldroch, S. Paradise, R. Vargo, R. West. Quality Assessment for MISR Level 2 Data. The Earth Observer, Vol. **8**(1), 19-21, January/ February 1996.

10.2 EOS PROGRAM

16. EOS General Instrument Interface Specification for the EOS Observatory (GIIS), GSFC 420-03-02, Rev. A, 01 December 1992.

17. The MODIS Calibration Plan, Version 2.0, GSFC, December 1995.

10.3 IN-FLIGHT CALIBRATION METHODOLOGIES

10.3.1 Kalman filtering

18. Freedman, E. and J. Byrne. Combining multiple sources for radiometric calibration of Landsat 7 using a Kalman filter. APRS, Part 5W1: ISPRS Intercommision Workshop, Vol. **30**, 272 - 278, 1995.

10.3.2 AVIRIS vicarious calibration

19. Green, Robert O. Determination of the Inflight Spectral Calibration of AVIRIS Using Atmospheric Absorption Features. Proc. Fifth Annual Airborne Earth Science Workshop, JPL Publication 95-1, 1995.

20. Green, Robert O. An Improved Spectral Calibration Requirement for AVIRIS. Proc. Fifth Annual Airborne Earth Science Workshop, JPL Publication 95-1, 1995.

21. Green, Robert O., James E. Conel, Mark Helmlinger, and Jeannette van den Bosch. Inflight Radiometric Calibration of AVIRIS in 1994. Proc. Fifth Annual Airborne Earth Science Workshop, JPL Publication 95-1, 1995.

22. Green, Robert O., M. C. Helmlinger, J. E. Conel, J. M. van den Bosch. Inflight Validation of the Calibration of the Airborne Visible/Infrared Imaging Spectrometer in 1993. Proc. Algorithm for Multispectral and Hyperspectral Imagery, SPIE **2231**, 1994.

23. van den Bosch, J. M., R. O. Green, J. E. Conel. Calibration of the Japanese Earth Resources Satellite-1 Optical Sensor Using the Airborne Visible/Infrared Imaging Spectrometer. Proc. Algorithm for Multispectral and Hyperspectral Imagery, SPIE **2231**, 1994.

24. Green, Robert O., James E. Conel, Mark Helmlinger, Jeannette van den Bosch, Chris Chovit and Thomas Chrien. Inflight Calibration of AVIRIS in 1992 and 199. Proc. Fourth Annual Airborne GeoScience Workshop, JPL Publication 93-26, 1993.

25. Green, Robert O. Use of Data from the AVIRIS Onboard Calibrator. Proc. Fourth Annual Airborne GeoScience Workshop. JPL Publication 93-26, 1993.

26. Green, Robert O., and Bo-Cai Gao. A Proposed Update to the Solar Irradiance Spectrum Used in LOWTRAN and MODTRAN. Proc. Fourth Annual Airborne GeoScience Workshop, JPL Publication 93-26, 1993.

27. Green, Robert O., James E. Conel, Jeannette van den Bosch, Masanobu Shimada, and Masao Nakai. On-orbit calibration of the Japanese Earth Resources Satellite-1 Optical Sensor using the Airborne Visible-Infrared Imaging Spectrometer. In *Optical Sensors and Calibration,* IGARSS'93, Tokyo Japan, 1993.

28. Green, Robert O., James E. Conel and Thomas G. Chrien. Airborne Visible-Infrared Imaging Spectrometer (AVIRIS): Sensor System, Inflight Calibration and Reflectance Calculation. International Symposium on Spectral Sensing Research, pp. 22, 1992

29. Green, Robert O., Steve Larson and Ian Novack. Calibration of AVIRIS digitized data. Proc. Third Annual Airborne Geoscience Workshop, JPL Publication 92-14, 1992.

30. Green, R. O. et al.. In-flight Calibration of the Spectral and Radiometric Characteristics of AVIRIS in 1991. Proc. Third Annual Airborne Geoscience Workshop, JPL Publication 92-14, 1992.

31. Green, R. O. and G. Vane. Validation/calibration of the Airborne Visible/Infrared Imaging Spectrometer (AVIRIS) in-flight. In *Conference on Aerospace Sensing, Imaging Spectroscopy of the Terrestrial Environment*. SPIE Orlando, Florida, 16-20 April 1990.

32. Chrien, T.G., R.O. Green, and M.L. Eastwood. Accuracy of the Spectral and Radiometric Laboratory Calibration of the Airborne Visible/Infrared Imaging Spectrometer, In *Proceedings of the Second Airborne Visible/INfrared Imaging Spectrometer (AVIRIS) Workshop*. JPL Publication 90-54, 1-14, 1990

33. Chrien, T. G., R. O. Green, and M. L. Eastwood. Accuracy of the Spectral and Radiometric Laboratory Calibration of the Airborne Visible/Infrared Imaging Spectrometer. In *Conference on Aerospace Sensing, Imaging Spectroscopy of the Terrestrial Environment*, SPIE Orlando, Florida, 16-20 April 1990.

34. Green, R.O., J.E. Conel, V. Carrere, C.J. Bruegge, J.S. Margolis, M.Rast, and G. Hoover. Determination of the in-flight spectral and radiometric characteristics of the airborne visible/ infrared imaging spectrometer (AVIRIS). In *Proceedings of the Second Airborne Visible/ Infrared Imaging Spectrometer (AVIRIS) Workshop*, JPL Publication 90-54, 15-34, 1990.

35. Green, R.O., J.E. Conel, V. Carrere, C.J. Bruegge, J.S. Margolis, M.Rast, and G. Hoover. Inflight validation and Calibration of the Spectral and Radiometric Characteristics of the airborne visible/infrared imaging spectrometer (AVIRIS). In *Conference on Aerospace Sensing, Imaging Spectroscopy of the Terrestrial Environment,* SPIE Orlando, Florida, 16-20 April 1990.

36. Green, R.O. Calibration of the Airborne Visible/Infrared imaging spectrometer (AVIRIS), Imaging Spectroscopy: Fundamentals and prospective applications. JRC, ISPRA, Italy, 23-27 October 1989.

37. Green, R.O. and G. Vane. In-flight determination of AVIRIS spectral, radiometric, spatial and signal-to-noise characteristics using atmospheric and surface measurements from the vicinity of the rare-earth-bearing carbonatite at Mountain Pass, California. In *Proceedings of the AVIRIS Performance Evaluation Workshop*, Gregg Vane, editor, JPL Publication, 1988.

38. Vane, G., T.G. Chrien, J.H. Reimer, R.O. Green, and J.E. Conel. Comparison of laboratory calibrations of the Airborne Visible/Infrared Imaging Spectrometer (AVIRIS) at the beginning and end of the first flight season. In *Conference on Recent Advances in Sensors, Radiometry and Data Processing for Remote Sensing*, SPIE Orlando, Florida, **924**,4-8 April 1988.

10.3.3 Histogram equalization

39. M. P. Weitreb, R. Xie, J. H. Lienesch and D. S. Crosby. Destriping GOES Images by Matching Empirical Distribution Functions. Remote Sens. of the Environ., **29**, 185 - 195, 1989.

40. M. P. Weitreb, R. Xie, J. H. Lienesch and D. S. Crosby. Removing Stripes in GOES Images by Matching Empirical Distribution Functions. NOAA Technical Memorandum NESDIS 26, National Oceanic and Atmosphere Administration, Washington, D. C., May 1989.

10.3.4 Coherent noise

41. Kieffer, H.H., E.M. Eliason, and P.S. Chavez, Jr. Intraband radiometric performance of the Landsat-4 Thematic Mapper. In *Landsat-4 Science Characterization Early Results, Vol. 3-Thematic Mapper (TM) Part 2 Early results Symposium*, NASA Conf. Pub. 2355, 22-24 February 1983.

42. Rice, D.P. and W.A. Malila. Investigation of radiometric properties of Landsat 4 MSS. In *Landsat-4 Science Characterization Early Results, Vol. 1-Multispectral Scanner (MSS) Early results Symposium*, NASA Conf. Pub. 2355, 22-24 February 1983.

10.3.5 Aliasing noise

43. Park, S.K and R. Hazra. Aliasing as noise: A quantitative and qualitative assessment. Technical Symposiums on Visual Information Processing II and Infrared Imaging Systems: Design and Testing IV, SPIE, 1993.

44. Park, S.K. Image gathering, interpolation and restoration: a fidelity analysis. Technical Symposium on Visual Information Processing, SPIE, 1992.

45. Park, S.K and S.E. Reichenbach. Digital image gathering and minimum mean-square error restoration. Technical Symposium on Visual Communications and Image Processing, SPIE, Vol. **1360**, 1990.

10.3.6 Desert scenes

46. Cosnefroy, H., X. Briottet, M. Leroy, P. Lecomte, R. Santer. In-field characterization of Saharan sites reflectances for the calibration of optical satellite sensors. IGARSS'94, Pasadena, 8-12Aug94, IEEE Catalog Number 94CH3378-7, 1500-1502, 1994.

10.4 MISCELLANEOUS

10.4.1 Exo-atmospheric solar irradiance

47. Wehrli, C. Extraterrestrial Solar Spectrum. World Radiation Center (WRC), Davos-Dorf, Switzerland, WRC Publication No. 615, July, 1985.

10.4.2 Radiative transfer

48. Hansen, J., and L.D. Travis. Light scattering in planetary atmospheres. Space Sci. Rev., **16**, 527-610, 1974.

10.4.3 Reflectance standards

49. Weidner, V.R., and J.J. Hsia. Reflection properties of pressed polytetrafluoroethylene powder. J. Opt. Soc. Am., **71**, 856-861, 1981.

APPENDIX A. NOMENCLATURE

The following definitions are used by the MISR IFRCC Team.

A.1 SCIENCE

equivalent reflectance. Radiometric requirements are defined at signal levels expressed as equivalent reflectances. This parameter is defined as:

$$\rho_{eq} = \pi L_\lambda / E_{0\lambda}$$

where L_λ is the spectral radiance incident at the sensor while observing a given target, and $E_{o\lambda}$ is the spectral exo-atmospheric solar irradiance at wavelength λ. (Both L_λ and $E_{o\lambda}$ are weighted by the passband response.) To convert an equivalent reflectance into radiance, therefore, $L_\lambda = E_{o\lambda} * \rho_{eq} / \pi$ where $E_{o\lambda}$ is the exo-atmospheric solar irradiance, as given by the following reference:

> Wehrli, C. Extraterrestrial Solar Spectrum. World Radiation Center (WRC), Davos-Dorf, Switzerland, WRC Publication No. 615, July, 1985.

With a single value, this parameter can be used to describe a spectrally dependent radiance level (e.g., the maximum radiance each MISR band should be designed to sense). It also gives the reader a more intuitive feel for the radiance level than if the radiance data itself were reported. This term is unique to MISR.

geophysical parameters. Those variables of the Earth's environment, including aspects of the land and water surfaces, atmosphere and space, which are used to describe the environment and geophysical processes. Geophysical parameters may be directly observable or deduced from sensor output as a higher level product.

observables. The fundamental physical quantity or quantities that a sensor can measure, such as temperature, which through a process of calibration can be related to a geophysical parameter. Observables can usually be measured by processes traceable to physical standards.

reflectance.

bidirectional reflectance factor (BRF). The ratio of radiance reflected by a sample to that which would be reflected into the same beam geometry by a lossless, lambertian surface that is identically irradiated. Thus, $R(\theta_i; \theta_r) = dL(\theta_r)/dL_{lam}(\theta_i;\theta_r) = \pi\, BRDF(\theta_i; \theta_r)$. Here θ_i and θ_r are the angles of incidence and reflectance, respectively. The MISR diffuse panel will be characterized in terms of reflectance factor.

bidirectional reflectance distribution function (BRDF). The BRDF is the ratio of that part of the radiance reflected into θ_r which originates from θ_i to the total irradiance from θ_i on the surface. Thus, $BRDF(\theta_i; \theta_r) = dL(\theta_r)/L_i(\theta_i;\theta_r) \cos(\theta_i) d\Omega$.

hemispheric reflectance, $\rho(\theta_i / h)$. This parameter is an integration of the BRDF over all reflectance angles. The symbol h denotes the integration of the reflected radiance over the hemisphere.

A.2 DATA

A.2.1 Data acquisition

camera configuration. The cameras have the capability to generate degraded resolution ground footprints by averaging adjacent samples (crosstrack) and successive lines (downtrack). Specific allocations of the averaging capabilities among the channels are referred to as camera configurations.

Global Mode (GM). A camera configuration (data averaging) mode capable of providing complete, continuous coverage of the sunlit Earth and consistent with the instrument power and data rate allocations.

Local Mode (LM). A camera observation mode in which high resolution images in all 4 bands of all 9 cameras of selected Earth targets are obtained by inhibiting pixel averaging in all bands of each of the cameras in sequence, one at a time, beginning with the first camera to acquire the target and ending with the last camera to view the target.

Calibration Mode (CM). An instrument mode in which the flight photodiodes are sampled at high data rates (25Hz), and transmitted with camera data. There are four such modes. For Cal-North and Cal-South, the diffuse panels are deployed and viewed by the cameras and photodiodes simultaneously. The forward and nadir cameras are calibrated at the North Pole, and the aftward and nadir cameras are calibrated at the South Pole. Each instrument channel in the cameras being calibrated is cycled through the spatial averaging modes (1 x 1, 1 x 4, and 4 x 4), as well as a sweep through all integration times. For Cal-Diode camera and diode data are acquired during Earth-observation; for Cal-Dark camera and diode data are acquired during dark-Earth (night) observations.

A.2.2 Data product generation

data product. The final processed data sets associated with the various measured and derived geophysical parameters which are the object of a specified investigation and referred to as a higher level product than the measurement provided by the instrument.

A.3 RADIOMETRIC PRODUCT

radiance conditioning. This process is used to adjust the camera measured radiances for imperfections in the camera design. Specifically, point-source function (PSF) data are used to reduce the effects of scattering within the focal plane, in-band scaling is done to adjust for in-band spectral profile nonuniformities with field angle and from one camera to another, and out-of-band response subtraction is included within MISR standard product generation.

radiance scaling. The process of converting DN data into a measure of incident spectral radiances, averaged over the MISR spectral response range.

A.4 CHARACTERIZATION

calibration. The set of operations which establish, under specified conditions, the radiometric, spectral, or geometric characterization of a sensor, as needed to understand the impact of the instrument performance on the data or the derived data products.

absolute calibration. The determination of calibration factors by comparison with a standard whose output is known in accepted physical (SI) units.

vicarious calibration (VC). The radiometric calibration of an in-orbit sensor through radiance determinations using in-situ or other transfer sensors (e.g., aircraft). Typically data are collected during an *intensive field-campaign*. The VC methodologies are:

1) high-altitude sensor-based calibration in which helicopter or aircraft sensors are used to map radiances and extrapolate to the required exo-atmospheric radiances;

2) surface radiance-based calibration in which atmospheric and surface-measured radiances are measured; or

3) surface reflectance-based calibration in which atmospheric and surface reflectance characteristics are measured by the field instruments.

For these methodologies, a radiative transfer code is used to extrapolate the observations to a top-of-atmosphere value. The magnitude of the atmospheric correction increases for approaches (1) through 3).

in-flight calibration. The calibration of an aircraft or satellite-based sensor while in flight. This may be through vicarious calibration exercises, or through use of an on-board calibration system.

preflight calibration. The calibration of a sensor prior to launch using laboratory standards.

relative calibration. The determination of the correction by comparison with a standard whose output is not necessarily known in physical units, but which is established in ratio or as a fraction of the value of the standard.

characterization. The measurement of the typical behavior of instrument properties which may affect the accuracy or quality of its response or derived data products.

cross-comparison. The process of assessing the relative accuracy and precision of response of two or more instruments. These activities are used to verify the calibration of the instruments involved.

Fidelity interval analysis. A statistical determination of the coefficients G and DN_o, along with their uncertainties, via an analyses such as that reported by

Chrien, N.C.L., C.J. Bruegge, and B.R. Barkstrom. Estimation of calibration uncertainties for the Multi-angle Imaging SpectroRadiometer (MISR) via fidelity intervals. In *Sensor Systems for the Early Earth Observing System Platforms*, Proc. SPIE **1939**, April, 1993.

These are the limits in radiance about the radiance estimated from the calibration regression, or the *fidelity intervals*

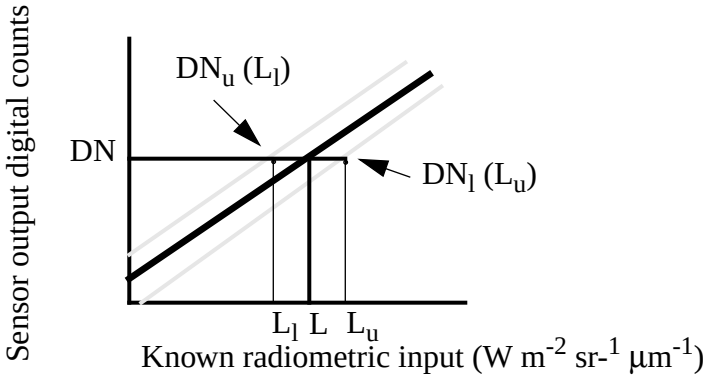

Radiometric transfer curve

traceability. The property of a result of a measurement whereby it can be related to appropriate standards, generally international or national standards, through an unbroken chain of comparisons.

verification. Tests and analyses to be performed during the design, development, assembly, and integration phases of an instrument to assure all instrument functional requirements have been met. Includes all sub-system and system tests done at the functional level. See *integrator verification tests*.

A.4.1 Radiometric

response coefficients. The coefficients of the radiometric calibration equation used to relate sensor output to incident radiance.

calibration equation. During radiometric calibration the relationship between an incident radiance field and camera digital output is established. The equation MISR will use is:

$$DN - DN_o = G_o + G_1 L_\lambda + G_2 L_\lambda^2 .$$

where

L_λ is the incident band-averaged spectral radiance, averaged over both in-and-out-of-band wavelengths, reported in units of [W m^{-2} sr^{-1} μm^{-1}], and defined by the equation:

$$L_\lambda = \frac{\int L_{source} \Re\lambda d\lambda}{\int \Re\lambda d\lambda}$$ and R is the relative instrument spectral response;

DN is the camera output digital number,

G_0, G_1, and G_2 are the response coefficients which, once determined, provide the radiometric calibration of a specific pixel,

DN_o is the DN offset, unique for each line of data, as determined by an average over the first eight "overclock" pixel elements.

photodiode laboratory standards. A set of commercially procured HQE photodiode standards used to establish the calibration of the MISR integrating sphere.

radiometric calibration. The determination of the response coefficients used in the calibration equation representation of a detector's responsivity. This is a flat-field determination, where use is made of a uniform target such as an integrating sphere or flight diffuse panel.

radiometric nomenclature. The International Commission on Illumination, CIE standards, have been adopted by the National Institute of Standards and Technology, Applied Optics, The Journal of the Optical Society of America, the Illuminating Engineering Society, and the American Society of Mechanical Engineers. MISR follows this nomenclature convention, as summarized in the table below.

Terms	Equations	Units
Radiant flux	$\Phi=\delta Q/\delta t$, Q=energy (J,erg)	W
Radiant density at a surface:		
Radiant exitance	$M=\delta\Phi/\delta A$	W m^{-2}
Irradiance	$E=\delta\Phi/\delta A$	W m^{-2}
Radiance	$L=\delta^2\Phi/\delta\Omega(\delta A\cos\theta)$	W m^{-2} sr^{-1}

In addition, spectral terms are denoted with a subscript λ, and have the additional units μm^{-1}.

radiometric transfer curve. The empirical observations of sensor output to incident radiance. The radiometric transfer curve is typically approximated by fitting to a calibration equation with linear, or higher order terms.

scene response. The determination of the optical PSF, scatter, pixel uniformity and other instrument characterizations from targets other than the uniform calibration targets.

A.5 INSTRUMENT

A.5.1 On-Board Calibrator

diffuse panel. The two diffuse panels are each an assembly within the mechanisms subsystem. The "North Pole Panel" swings aft during calibration to calibrate the forward and

nadir cameras. The “South Pole Panel” swings forward during calibration to calibrate the aftward-looking and nadir cameras. The panels are used to reflect solar light into the cameras, and calibration photodiodes. The exitant radiance emitted from the panels is known through the photodiode measurements. A diffuse panel is deployed or stowed.

goniometer. The goniometer is an assembly within the mechanisms subsystem. Functionally it serves as one element to the OBC. The goniometer consists of one PIN photodiode subassembly, denoted the G-PIN, as well as a motor, arm, and electronics subassemblies. This G-PIN contains four radiation resistent photodiode components, each filtered to one of the four MISR wavelength channels. These diode components are identical to all other PIN diodes. The goniometer can be in one of three states: *on*, *running*, or *off*.

The goniometer provides a measure of the diffuse panel angular reflectance stability. It is limited with respect to this goal, in that coverage is only along one slice of the reflecting hemisphere. The angles used in this design, however, cover the extremes of camera view angles, and include the near-nadir view of the D-cameras, and most oblique view of the An-camera.

On-Board Calibrator (OBC). The diffuse panel, photodiode, and goniometer assemblies which provide a relative and absolute radiometric calibration of the nine cameras while in flight. The OBC is not delivered as a discrete subsystem.

photodiode standards.

high quantum efficient (HQE). The HQE photodiodes are nadir-viewing. They are denoted 1-HQE, 2-HQE, 3-HQE, and 4-HQE and are the Band 1 to Band 4 spectrally filtered assemblies. Each package contains three photodiodes in a trapped configuration, plus a single spectral filter in a hermetic package. Precision apertures define the viewing solid angle.

PIN. The bench-mounted PIN diodes are an assembly within the analog electronics subsystem. They consist of a Df-PIN which has the same Earth-view angle as the Df camera, the Da-PIN, or photodiode which looks in the Da camera direction. Additionally, there are two An-PIN diodes. PIN photodiodes are of a “p-type” plus “intrinsic layer” plus “n-type” silicon, hence the name. PIN photodiodes are more radiation resistent than the HQE photodiodes. Each PIN package consists of a single photodiode and a single spectral filter in a hermetic package. Precision apertures define the viewing solid angle.

APPENDIX B. CALIBRATION MODE SEQUENCE

Routine calibrations of MISR are conducted using Cal-North, Cal-South, and Cal-Dark sequences, all conducted in a single orbit. The first of these is depicted in Figure B.1. The Cal-North and Cal-South are also detailed in Table B.1. In addition, there exists a Cal-Diode mode, which proceeds with the cameras configured as for a Global Mode survey. Here the photodiodes and cameras simultaneously view the day-lit Earth.

Table B.1. Polar calibration sequences.

Step	Cal-North	Cal-South
1	Da, Ca, Ba, Aa, An ON	Df, Cf, Bf, Af, An ON
2	Photodiodes on	Photodiodes ON
3	Collect *dark Earth* data (prior to sunrise)	Deploy South Pole diffuse panel (-x)
4	Stop photodiode data acquisition	Collect *above atmosphere* data
5	Stop camera data acquisition (keeping electronics on)	Goniometer on
6	Deploy North Pole diffuse panel (+x)	Collect *above atmosphere* data
7	Continue camera and photodiode data acquisition	Collect *sunset* data
8	Collect *dark panel* data (prior to sunrise)	Goniometer off. Continue data collection
9	Collect *sunrise* data (Sun viewed through Earth's atmosphere)	
10	Goniometer on (continue data collection)	
11	Collect *above atmosphere* data (no atmospheric attenuation)	Collect dark panel data
12	Goniometer off (continue data collection)	Photodiodes off
13	Photodiodes off	Stow diffuse panel
14	Stop camera data acquisition	Collect *dark Earth* data
15	Stow diffuse panel	Cameras powered off in order

Figure B.1. Cal-North calibration sequences.

In Cal-Dark data are acquired over the dark Earth, near the equator over ocean targets. The calibration panels are stowed. All nine cameras and diodes are turned on one minute prior to data acquisition. The sequence begins with the nadir and fore cameras acquiring data for about one and a half minutes, followed by nadir and aft-camera data acquisition for an additional one and a half minutes. Thereafter all cameras and diodes are turned off. For this sequence the goniometer is off, although the ability to commanded on is available.

During the Cal-North, Cal-South, and Cal-Dark Calibration Mode sequences, the camera's will be commanded into several camera configurations, as described in this section. The two primary configurations are termed *Config. 1x1* and *Config. Home Run*. In Config. 1x1 five camera collect data simultaneously (either the fore- plus nadir or aft- plus nadir cameras). Four of these cameras are in 1x1 (unaveraged data), with a fifth camera in a 4x4 averaging mode. (Only 18 channels can be in high resolution at any one time, so as not to violate the 8.5 Mbit s^{-1} orbital peak data rate. The Calibration Mode would be simplified if 20 simultaneous high resolution channels were permitted.) The specific camera in this 4x4 state sequences amongst the five cameras involved.

In Config. Home Run five cameras also collect data simultaneously. Here, however, the camera configurations changes amongst three data modes. This is best summarized by a series of tables, given below.

Table B.2. Camera sequences and configurations during Calibration Mode

Sequence name	Camera configuration	Time (min)	Comments
Cal-North, Cal-South, and Cal-Dark sequence			• New moon • Monthly, except five times during A&E period • All sequences are in same orbit
Cal-North			• +x diffuse panel deployed • Aft + nadir cameras calibrated (5 camera data acquisition) • Warm up 5 cameras before cal data acquisition.
	1x1	5.0	• Used during - *dark Earth* and *dark panel* windows (no Sun illumination onto the panel), - *with atmosphere* window (Sun-panel path goes passes through the Earth's atmosphere), and - *above atmosphere* window (no Earth atmosphere path; best sun illumination angle). • Goniometer may be on or off
	Home Run	1.5	• *With atmosphere* window • Goniometer may be on or off

Table B.2. Camera sequences and configurations during Calibration Mode

Sequence name	Camera configuration	Time (min)	Comments
Cal-South			• -x diffuse panel deployed • Fore+nadir cameras calibrated (5 camera data acquisition)
	1x1	5.0	• See Cal-North comments
	Home Run	1.5	• See Cal-North comments
Cal-Dark	Home Run	3.0	• Data acquisition over *dark Earth* • Perform first for aft + nadir cam (1.5 min), followed by fore + nadir cam (1.5 min) • Diffuse panel stowed • Conduct just prior to Cal-North • 9 cameras on 5 min before data acquisition. • Diodes on 1 min before data acquisition. • Goniometer may be on or off

Table B.3 defines the 1x1 configuration. Only 1x1 data in this configuration is used to determine a channels radiometric calibration parameters.

Table B.3. Camera configuration 1x1

Line Repeat No. (40.8 msec/ line)	An	A	B	C	D
1	1x1	4x4	1x1	1x1	1x1
17	1x1	1x1	4x4	1x1	1x1
33	1x1	1x1	1x1	4x4	1x1
49	1x1	1x1	1x1	1x1	4x4

Total time/ cycle: 64 lines * 40.8 msec = 2.6 sec ~ 0.04 min. Repeat for desired time window.

When this configuration is used during Cal-North the aftward plus nadir cameras collect data. When this configuration is used during Cal-South the forward plus nadir camera collect data.

Config. Home Run is a commanding of the four camera configurations steps, in turn. It is intended that this ordering be preserved.

Table B.4. Config. Home Run steps

Configuration step	Time (sec)	Comments
Integration Time Ramp	41.8	• Provides data at all allowable integration times • Restore to mission integration time once complete
Averaging Step	7.8	• Provides data in all data averaging modes
1x1	10.4	• Same as 4 cycles of *Config. 1x1*
Accelerated Local Mode Step	32.6	• Global Mode with 1x1 cycling through 9 cameras • provides data in science camera configuration

Total time: 92.6 sec = 1.5 min.

Table B.5 defines the Integration Time Ramp step. These data will be used to verify camera electronic health.

Table B.5. Integration Time Ramp step

Sample no. (0.1632 sec/ frame)	CCD integration time (all channels)
1	t_{min}
2	$t_{min}+\delta t$
3	$t_{min}+2*\delta t$
(n-1)4+1	$t_{min}+(n-1)*\delta t$
256	$t_{min}+255*\delta t$

Total time: 256 * 0.1632 sec/ frame= 41.78 sec ~ 0.70 min.

Table B.6 defines the Averaging Step. These data will be used to verify calibration gain and offset coefficients, as needed for all Averaging Modes, can be computed from the 1x1 high resolution data.

Table B.6. Averaging Mode Step

Line Repeat No. (40.8 msec/ line)	An	A	B	C	D
1	1x1	1x1	4x4	1x1	1x1
32	1x1	1x1	1x1	4x4	1x1
65	1x4	1x4	1x4	1x4	1x4
129	4x4	4x4	4x4	4x4	4x4

Note: Total time = 192 lines * 40.8 msec = 7.83 sec = 0.13 min.

Here the cameras are sequenced between data averaging modes. The first four cases in this table are needed to collect unaveraged data over the poles. Because of the limited peak data rate, I believe only 18 channels can be in 1x1 at any one time (we need 20 channels to collect unaveraged data simultaneously).

Table B.7 defines the Local Mode Step. These data are used to verify the instrument response in Science Local Mode. The instrument output in this Step should be predictable from the 1x1 response data.

Table B.7. Accelerated Local Mode Step - High resolution D camera

Band/ Camera	An	A	B	C	D
1 (Blue)	1x1	4x4	4x4	4x4	1x1
2 (Green)	1x1	4x4	4x4	4x4	1x1
3 (Red)	1x1	1x1	1x1	1x1	1x1
4 (Near-IR)	1x1	4x4	4x4	4x4	1x1

Repeat for 200 line repeat times, then

Table B.8. -High resolution C camera

Band/ Camera	An	A	B	C	D
1 (Blue)	1x1	4x4	4x4	1x1	4x4
2 (Green)	1x1	4x4	4x4	1x1	4x4
3 (Red)	1x1	1x1	1x1	1x1	1x1
4 (Near-IR)	1x1	4x4	4x4	1x1	4x4

Repeat for 200 line repeat times, then

Table B.9. -High resolution B camera

Band/ Camera	An	A	B	C	D
1 (Blue)	1x1	4x4	1x1	4x4	4x4
2 (Green)	1x1	4x4	1x1	4x4	4x4
3 (Red)	1x1	1x1	1x1	1x1	1x1
4 (Near-IR)	1x1	4x4	1x1	4x4	4x4

Repeat for 200 line repeat times, then

Table B.10. -High resolution A nadir camera

Band/ Camera	An	A	B	C	D
1 (Blue)	1x1	1x1	4x4	4x4	4x4
2 (Green)	1x1	1x1	4x4	4x4	4x4
3 (Red)	1x1	1x1	1x1	1x1	1x1
4 (Near-IR)	1x1	1x1	4x4	4x4	4x4

For a total time of four steps * 40.8 msec/ line *200 lines = 32.6 sec = 0.54 min

When this configuration is used during Cal-North the aftward plus nadir cameras collect data. When this configuration is used during Cal-South the forward plus nadir camera collect data.

The goniometer shall run for 1 minute during the Above Atmosphere windows, starting (or stopping) at the With Atmosphere window boundary. It will run for 10 cycles (about 1 minute). It is desirable to not run the goniometer during the entire calibration window, in case motor noise disturbs the camera and photodiode measurements. The activation of the goniometer is not limited because of the uncompensated momentum requirement. There is some loss of science data, however, due to the uncompensated momentum requirement.

B. Calibration mode sequences